Top Curr Chem (2015) 364: 183–224
DOI: 10.1007/128_2014_578

Published online: 12 March 2015

Spectroscopy of Metal-Ion Complexes with Peptide-Related Ligands

Robert C. Dunbar

Abstract With new experimental tools and techniques developing rapidly, spectroscopic approaches to characterizing gas-phase metal ion complexes have emerged as a lively area of current research, with particular emphasis on structural and conformational information. The present review gives detailed attention to the metal-ion complexes of amino acids (and simple derivatives), much of whose study has focused on the question of charge-solvation vs salt-bridge modes of complexation. Alkali metal ions have been most frequently examined, but work with other metal ions is discussed to the extent to which they have been studied. The majority of work has been with simple cationic metal ion complexes, while recent excursions into deprotonated complexes, anionic complexes, and dimer complexes are also of interest. Interest is growing in complexes of small peptides, which are discussed both in the context of possible zwitterion formation as a charge-solvation alternative, and of the alternative metal-ion bond formation to amide nitrogens in structures involving iminol tautomerization. The small amount of work on complexes of large peptides and proteins is considered, as are the structural consequences of solvation of the gas-phase complexes. Spectroscopy in the visible/UV wavelength region has seen less attention than the IR region for structure determination of gas-phase metal-ion complexes; the state of this field is briefly reviewed.

Keywords Action spectroscopy · Amino acids · Gas phase ion structures · Metal ion complexes · Peptides

R.C. Dunbar (✉)
Chemistry Department, Case Western Reserve University, Cleveland, OH 44106, USA
e-mail: rcd@po.cwru.edu

Contents

1 Introduction

Ionic complexes can be built by assembling one or more ligands around an ionic core, where the core may be a proton, a metal ion, or a more complicated ion (cluster ion, inorganic ion, etc.). Such structures can have biological interest and relevance when the ligand(s) wrapping around the ionic core comprises the stuff of living systems, and here we are interested specifically in the structures formed when the wrappings are essentially peptides and the core is a metal ion.

The convergence of remarkable technological developments on several fronts has quite suddenly made spectroscopic characterization of gas phase ions greatly more powerful, convenient and versatile (see Oomens [1]), with the result that the last decade has seen a flowering of ion spectroscopy. A major portion of the hundreds of publications in this area has addressed ionic complexes, and a large number of these reports in the last few years have had at least passing relevance to biological, biochemical and biophysical concerns. Such is the focus of the present survey. A number of reviews touching on this area have appeared in the last few years [2–9].

Interesting questions arise when the ligand is complex enough to offer a choice of binding sites and binding geometries as it arranges around the core. Answers to such questions can then reflect back to the native condensed-phase biological architecture to enhance understanding of the structure of metallic charge sites in living systems.

The flavor of the present chapter overviewing the field might be suggested by Fig. 1, which lays out in skeletal form the progression from spectroscopy of the simplest "peptide" complexes (amino acids), through small oligopeptides (here, a dipeptide), to large systems (proteins). The simplest systems show a few prominent spectroscopic features which can readily be identified (with computational help) with specific molecular surface groups (here, vibrations associated with the C-terminus). The dipeptide emphasizes the initial emergence of the spectroscopic signatures (still individually discrete) reflecting the body of the peptide (the amide linkages and the interior residue side chains); finally, the complex of the large cytochrome-c peptide [13] shows the complete submergence of the C-terminal features, leaving the spectrum dominated by the two amide bands of the 100 or

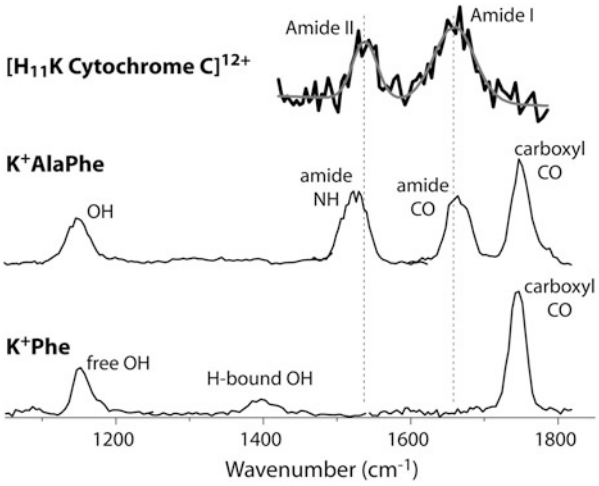

Fig. 1 Infrared photodissociation action spectra in the fingerprint infrared region from fairly early in the modern evolution of spectroscopy of biologically interesting complex ions. These spectra illustrate the use of electrospray ion production, ion trapping mass spectrometry (Fourier-transform ion cyclotron resonance in these examples) and the FELIX free electron laser light source. Lower spectrum originally derived from [10, 11]; middle spectrum from [12]; upper spectrum from [13]. Figure reproduced with permission from [12]

so amide linkages, just as with proteins in solution. Our survey follows the same path from smaller to larger ligands, first in some detail for the infrared (vibrational) spectral domain, and then more briefly for the less well developed domain of electronic (visible/ultraviolet) spectra.

Parallel to our survey of peptide metal complexes, which is encompassed by the present chapter, are a large number of spectroscopic structure studies of protonated amino acids and peptides (for example, amino acids and derivatives [14–29] and larger peptides [30–38]). We could consider the proton as a metal ion and weave the spectroscopy of protonated peptides into our discussion here, but we largely leave such a survey for another place. More broadly, spectroscopic information is becoming pervasive in the study of gas-phase biomolecules, and many further examples appear in other chapters in this volume. One of the exciting frontiers is the spectroscopy of cryogenic ions [39]. Not much has been reported yet in this latter domain about metal-ion complexes of biomolecules, but we can expect such cold ion spectroscopy to be a flourishing area in the near future. The present state of this area is well covered in the chapter of Boyarkin and Rizzo in this volume [40]. Yet another frontier area not explored in the present chapter is the observation and exploitation of gas-phase ion fluorescence [41], where some especially noteworthy recent work is bringing to bear the powerful tool of FRET (Fluorescence Resonant Energy Transfer) for characterization of large biomolecules [42, 43].

2 Infrared and Vibrational Spectroscopy

2.1 Amino Acids and Derivatives

2.1.1 Charge-Solvated vs Salt Bridge (Zwitterion)

Forming a bedrock for the understanding of metal-ion peptide interactions, great effort has gone into the study of metal-ion binding to gas-phase amino acids. A principal theme arises from the observation that the natural amino acids self-ionize to the zwitterionic form in aqueous solution (Scheme 1), while in gas phase their most stable form is the canonical conformation. It was natural to ask whether interaction with a metal ion in gas phase could preferentially stabilize the zwitterionic conformation of the amino acid ligand to make this the most favorable conformation. The answer to this question has been explored by now in considerable depth, revealing a delicately balanced and multifaceted interplay of factors which may or may not favor isomerization of the ligand to the zwitterionic form. Early on, the Bowers group [44] explored this question both experimentally, using largely inconclusive evidence from collision cross sections, and computationally. Starting in the mid-1990s, Williams' group pioneered the use of black-body infrared dissociation (BIRD) to address ion-structure investigation, including the present question (see [45] for one example). Near the beginning of this century, the Armentrout group began to use the high-quality thermochemical information about ion dissociation pathways coming from guided ion beam mass spectrometry (GBIMS) to address this question (for example, [46]), and they continue to use this approach extensively as a complementary technique to their spectroscopic studies. These and other experimental programs, along with widespread computational study, formed a backdrop of understanding of the issue. Realization that spectroscopy could provide more conclusive evidence than other experimental approaches [47] launched a decade of IR action spectroscopy centered around this theme.

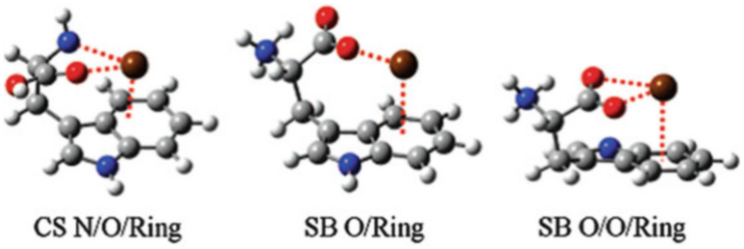

Scheme 1 Low-energy structures for the complex of Ba^{2+} and Trp. Structures can be classified as salt-bridge (SB: interaction between the positive metal ion and the negative carboxylate of the zwitterionic amino acid) or charge solvation (CS: interaction of the metal ion with Lewis-basic sites of the canonical amino acid). Nomenclature of the various structures further includes the main binding sites of the amino acid

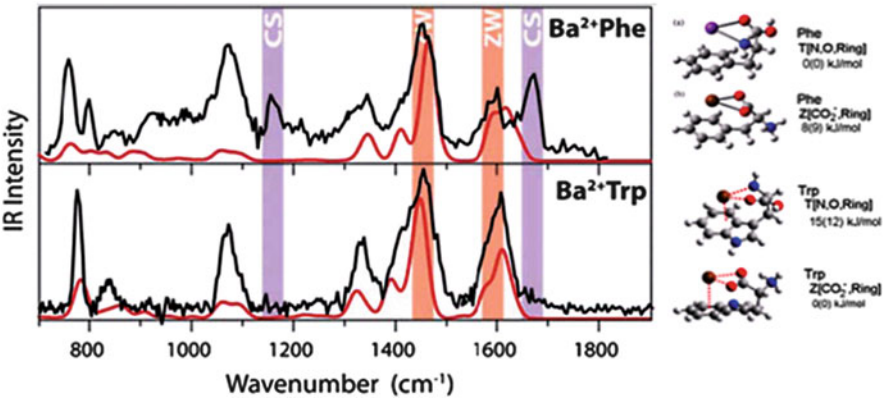

Fig. 2 Spectra of the trapped populations of Phe and Trp complexes of Ba^{2+} (figure adapted from [11]). Comparison of the IRMPD spectra (*upper trace* in each panel) of the Ba^{2+} complexes of Phe and Trp. The *lower* (*red*) trace in each panel shows the calculated spectrum of the SB conformation, and two expected diagnostic features for the Z[CO_2^-,Ring] (SB) conformation are designated by the (*orange*) bars labeled ZW. Two diagnostic features expected for the T[N,O,Ring] charge-solvated conformation are designated by the (*purple*) bars labeled CS, and are seen to be present in the observed spectra only in the Phe case

As an example of the strength of this tool for characterizing the populations of the electrosprayed, trapped ionic complexes, Fig. 2 contrasts spectra of the Ba^{2+} complexes of the two closely related amino acids Phe and Trp [11]. It is clear that the Trp complex is homogeneously SB, but for the Phe case the CS conformation has comparable stability leading to a mixture of both conformations with substantial abundance of each. Figures 1 and 2 underscore the strength of this structure-determining tool in circumstances where we can identify effective diagnostic features in the spectrum. In these examples of CS/SB identification for amino acid ligands, the diagnostic peaks for both conformations are clearly evident. Figure 1 (lowest trace) shows an uncontaminated CS complex with the characteristic markers of the carboxylic acid stretch band at short wavelength (above 1,700 cm^{-1} for singly charged metals) and OH bending mode at 1,150 cm^{-1}. These are absent for the uncontaminated SB complex in Fig. 2 (lower trace), and these spectral regions are quite empty in the latter spectrum. Conversely, the characteristic markers for SB amino acids, the asymmetric carboxylate COO^- stretch (1,600 cm^{-1}) and the $-NH_3^+$ bend (between 1,400 and 1,450 cm^{-1}), are completely absent in these empty spectral regions for K^+Phe in Fig. 1.

One would like to draw quantitative conclusions about the relative abundances of the conformations from the sizes of the peaks in Fig. 2 (upper trace), but this is unjustifiable for several reasons. For one thing, the one-photon optical absorption strengths of the different peaks as calculated quantum-mechanically do not correspond accurately to the effective multiphoton absorption cross sections appropriate to the IRMPD process [8]. For another, as clearly demonstrated by Prell et al. [48] among others, the time course of IRMPD dissociation can differ widely for different

isomers, so that measurements at a single laser irradiation time (as is usually the practice) can be quantitatively misleading.

The early focus of this field was a simple binary decision of whether the given metal-ion/amino-acid pair gave a ground state complex with canonical or zwitterionic character. From a simple point of view, the canonical form is stabilized by the local solvation of the metal ion by surrounding ligand (shielding its charge from the vacuum), while the zwitterion is stabilized by electrostatic interactions in the form of a (+ − +) salt bridge. Thus, these two forms are commonly referred to respectively as "charge-solvated (CS)" or "salt-bridge (SB)" conformations. (Since the salt-bridge commonly involves a zwitterionic (ZW) form of the ligand, the designations SB and ZW can be taken as interchangeable in much of this literature). A review 4 years ago [5] summarized the evidence at that time, displayed in a comprehensive matrix of metal-ion/amino-acid pairs. Since then, it has become increasingly clear that a binary CS vs SB decision is too simple, and the combination of computation with spectroscopy has revealed trends governed by more subtle considerations. Table 1 presents an update of their matrix, displaying the spectroscopically determined evidence as of mid-2013. There is a useful update specifically of the computed CS/SB preferences for alkali metal ions in [62] (Fig. 7).

With the bias that spectroscopic assignments are the most definitive experimental evidence of which isomers are actually formed and observed under given instrumental conditions, we have focused our table primarily on structures assigned from spectroscopic data. Computation can now often predict the relative stabilities of different isomers with good confidence, but a full survey and evaluation of this extensive computational literature is beyond our scope. In order to clarify trends, we have included in our table some cases, indicated by square brackets, where theory or alternative experimental approaches are the only evidence so far available. We have ordered the metal ions within each charge state by a computed chelation-length parameter, which is akin to the standard ionic radius, but perhaps more appropriate for these chelation complexes. The amino acids are ordered according to their binding affinity for Na^+ [49], based on the observation that SB/CS preferences in tryptophan appeared to correlate well with this parameter [77].

Several basic structure types often compete to determine the ground state, as illustrated for Rb^+Ser in Scheme 2, where we have designated the isomers using the letter coding of Table 1, along with the square-bracket descriptive coding used by the Armentrout group. These basic structure themes can be summarized as follows:

1. T. Tridentate Chelating CS. T[CO,N,X] where the ligand chelates the metal through three Lewis-basic sites (X being a side-chain Lewis-basic atom)
2. B. Bidentate Chelating CS. B[CO,N] or B[CO,X] where the metal ion is chelated at only two sites
3. C. C-Terminal CS. Metal coordinated to COOH group, C[COOH] or C[COOH, X]. Metal ion coordinates both oxygens of the C-terminal COOH group without formation of a zwitterion
4. Z. Salt Bridge SB, (Zwitterion). COOH deprotonates to give zwitterion, Z [CO_2^-]

Table 1 Amino acid binding modes

AA	D‡	H^+	Li^+	Na^+	Ag^+	K^+	Rb^+	Cs^+	Mn^{2+}	Ca^{2+}	Ba^{2+}
R§			1.94	2.31	2.52	2.66	2.86	3.03	2.08[a]	2.28	2.60
Gly	161	[B[mm]]		[B,X[q,c]]	[B[v]]	[B[w]]	[C[q]]	[C[x]]	[Z[a]]	[Z[jj,kk]]	Z[f]
Ala	167	[B[mm]]		[B[q]]	[B[v]]		[C[q]]		[Z[a]]		
Val	173	[B[mm]]	[B[ff]]	[B[ff]]	[B[v]]				[Z[a]]		Z[s]
Cys	175	B[g]	T[g]	T[g]	[T[v]]	C[g]	C[g]	C[g]	[T[a]]		
Leu	175	[B[mm]]			[B[v]]				[Z[a]]		
Ile	176	[B[mm]]			[B[v]]				[Z[a]]		
Pro	196	[B[mm]]	Z[r]	Z[c]	[Z[v]]	Z,C[r]	Z,C[r]	Z,C[r]	[Z[a]]	[Z[ee]]	Z[s]
Ser	192	[B[mm]]	T[h]	T[h]	[T[v]]	T,C[h]	T,C[h]	T,C,Z[h,t]	[T[a]]		Z[s]
Thr	197	[B[mm]]	T[l]	T[l]	[T[v]]	T,C[l]	T,C[l]	T,C,Z[l]	[T[a]]		
Met	197	T[m]	T[m]	T[m]	[T[v]]	T,C[m]	T,C[m]	T,C,Z[m]	[T[a]]		
Phe	198	B[cc]	T[n]	T[n]	T[n]	T[hh,n]	T,B[n]	T,C[n]	[T[a]]		Z,T[n]
Tyr	201	B[cc]			[T[v]]	T[hh]			[T[a]]		
Asp	203	[B[mm]]	T[p]		[T[v]]			C'[p]	[T[a]]		Z[p]
Glu	204	B[p]	T[p]		[T[v]]			B[p]	[T[a]]	Z[p]	Z[p]
Trp	210	B[dd]	T[o]	T,B[o]	T[o,ii]	T,B[o]	T,B[o]	T,B[o]	[T[a]]		Z[ll]
Asn	206	B[f]	T[f]	T[f]	[T[v]]	T,C[f]	T,C[f]	T,C[f]	[T[a]]		T[f]
Gln	212	B[d]	T[d]	T[d]	[T[v]]	T,B[d]		T,X[d]	[T[a]]	Z[p]	Z[s]
Lys	>213	B[i]	T[i]	T[i]	[T[v]]	B[i]			[T[b]]		
His	219	B[bb]	T[j]	T[j,k]	[T[v]]	B,T,C[j]	B,T,C[j]	B,T,C[j]	[T[b]]	Z,T[j,k]	Z[k]
Arg	>225	B[e]	T[e]	Z,T[e,t]	B[e]	Z[e]	Z[e]	Z[e]	[T[a]]		Z[s]

‡ D = amino acid binding energy to Na^+ (kJ/mol) (Ref. [49]). Note that most of these kinetic-method binding energies have been remeasured subsequently by other techniques like guided beam dissociation, and the values listed here should not be taken as definitive. In particular, Asp [50] and Pro [51] are most likely lower by the order of 10 kJ mol^{-1}

§ R = B3LYP distance from metal to carbonyl O in M^+alanine (Å)

[Square brackets] = theory or non-spectroscopic experiment

Color coding:

Red=CS Blue=SB Purple=mixed CS and Z

Letter coding:

T=Tridentate CS B=Bidentate CS (CO,X) C=CS (COOH) C'=CS (COOH plus additional site) Z=SB X=unidentified CS ligand

a [52], b [53], c [46, 47], d [54], e [15, 20], f [21], g [18], h [55], i [14, 56], j [57], k [58], l [59], m [16], n [11], o [60], p [61], q [44], r [62, 63], s [64], t [48], u [65], v [66], w [67], x [68], aa [69], bb[17], cc [70], dd [39], ee [71], ff [72], gg [73], hh [10], ii [74], jj [75], kk [76], ll [77], mm [78]

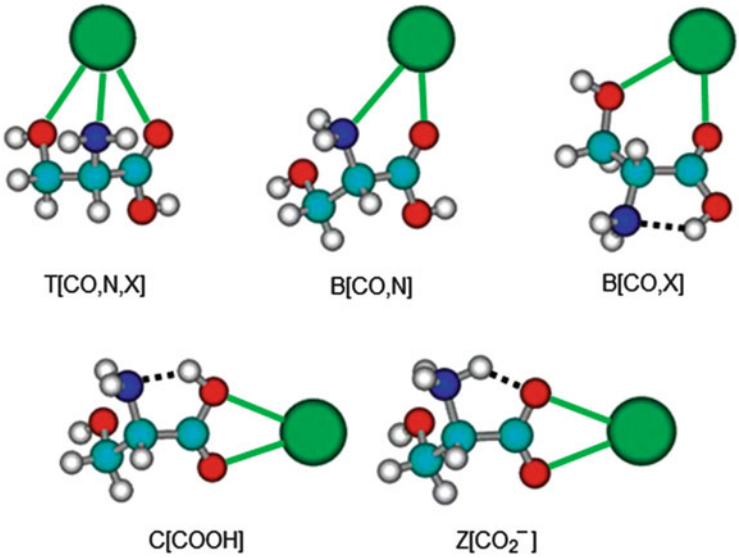

Scheme 2 Structures of the principal isomers of metal-ion serine complexes. Reproduced with permission from [55]

Some trends can be seen in Table 1, which are developed and explored extensively in the literature. Although there are occasional exceptions to most of these trends, the following principles seem to be mostly valid for understanding and predicting the relative stabilities of the different binding motifs described here:

1. Effect of metal size on choice among the three likely CS binding motifs B, T, and C. Small metals gain more from solvation, which enhances more highly solvated CS forms. Thus T and B are favored over C for small metals, and T is favored over B for small metals. (There is effectively no possibility of a T conformation for the aliphatic amino acids Gly, Ala, Val, Leu, Ile, and Pro.)
2. Effect of metal size on CS vs SB preferences. Other things being equal, small ion size is more favorable to CS stabilization (T, B, or C) by local micro-solvation of the bare metal ion, while large metal ion size reduces the micro-solvation energy gain to the point that SB stabilization (Z) becomes competitive. Thus it is among the larger metal ions that we find increasingly frequent cases of Z ions in the population. (Pro and Arg are exceptional cases often preferring Z, because of the availability of a nitrogen site with abnormally high proton affinity to attract the carboxyl proton.)
3. Effect of metal size, ion charge, and nitrogen-site basicity specifically for the choice between C[COOH] and Z[CO_2^-]. An important point is that C[COOH] converts into Z[CO_2^-] by simple displacement of the carboxyl proton through a short distance, which has the result of charge separation into the salt-bridge configuration. Some circumstances make the salt-bridge-forming position of the proton in Z better than the neutral proton position in C, namely (1) the metal ion is large (disfavoring CS microsolvation), (2) the charge is high (doubly charged

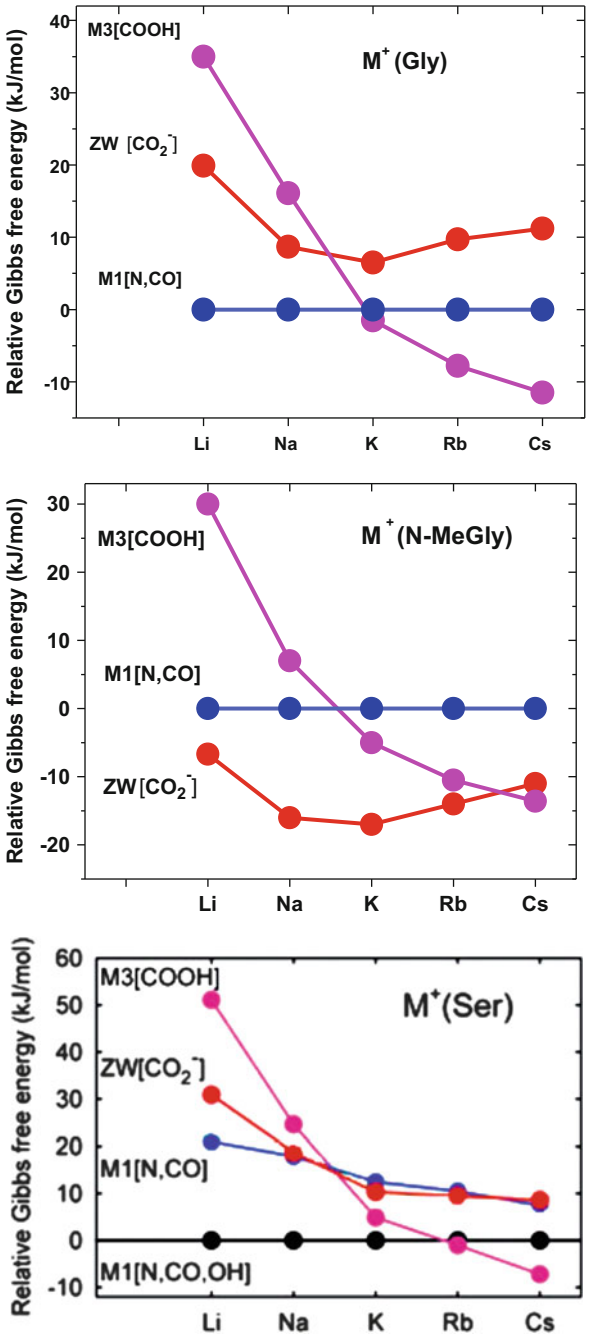

Fig. 3 Trends of the important isomers as a function of metal size for three different amino acids. Computational results plotted from [55] and [62]

metals), and (3) the proton-accepting site is strongly basic (Pro, Arg, N-methyl derivatives). A zwitterion ground state is more likely given any of these conditions.

4. Effect of ion charge on CS/SB preference. Higher charge on the metal enhances all binding interactions, but apparently favors the SB electrostatic stabilization associated with the salt bridge more strongly than the ion-solvation interactions leading to CS. Except for the special cases of Pro and Arg, all of the strongly favored SB ground states in Table 1 are doubly charged.

As an illustration of the interplay of factors across the alkali metals, Fig. 3 shows the shifting energies of the principal players for glycine [62] (where there is no side chain) and for serine [55] (as a representative amino acid where side-chain interactions play a role). Two effects are notable when the side chain is introduced in going from Gly to Ser: (1) the new CS tridentate structure T[N,CO,OH] appears and is dominant for smaller metal ions, and (2) the stability of Z[CO_2^-] zwitterion is greatly enhanced because the electronegative side chain can participate in extended salt bridge stabilization. However, the CS structure C[COOH] dominates in both cases for large metal ions. Moision and Armentrout showed by experiment and computation [67] that the small alkali metals favor binding to the NH_2 group, while the larger alkali metals switch to a preference for binding to the more extended carboxyl terminal COOH group. This principle rationalizes the switch from B or T toward C in going from Li^+ across to Cs^+ for many amino acids in the table.

Turning the nitrogen from primary to secondary amine increases its local basicity, and has been shown in many examples to enhance the tendency to separate charge and form an SB salt bridge by moving an acidic proton to this site. Methylation increases the stability of the SB form relative to CS forms by significant amounts (~15–20 kJ/mol) [14, 56, 62]. This often results in SB replacing CS as the ground state in N-methylated derivatives, and also results in the exceptional appearance of SB for most proline complexes. The effect has been frequently verified both computationally and spectroscopically through methylating this nitrogen in primary aliphatic amino acids, as in [54, 62]. The effect is nicely exemplified by the calculations of [62] shown in Fig. 3b. Comparing the plots for glycine vs *N*-methylglycine, it is seen that the effect of methylation is primarily to stabilize the zwitterion by about 20 kJ/mol relative to the other conformations. The Williams group noted a redoubled effect with two methyl substituents, giving the first spectroscopically characterized Li^+ amino acid complex with SB conformation (lysine) [56].

Trends comparing aliphatic amino acids with those having active side chains were originally noted by Wyttenbach et al. [44]) and were recently clarified by Drayss et al. [62]. Computationally, the aliphatic amino acids show a trend toward greater relative CS stability with increasing size of alkali metal ions, while the opposite trend, with SB being increasingly favored for larger metal ions, is observed in amino acids with active side chains. This apparent discrepancy is not real, because in the aliphatic cases, the stable CS structure which is favored in comparison with SB for large metal ions is the C-terminal C[COOH] or C[COOH,X] structure, whereas in the active side chain cases, it is a chelated bidentate B[CO,X] or tridentate T[CO,N,X] conformation which is in competition with the SB conformation. This situation is all illustrated computationally in Fig. 3. For the natural

amino acids, these trends of CS vs SB character are not usually observable experimentally (not counting the exceptional cases of Pro and Arg), because one or another CS structure is usually more stable than SB so that CS is observed as the ground state in all cases, but various studies [14, 62, 80] have displayed IRMPD evidence for SB preferences using methyl-substituted amino acids, where the basicity of an amino nitrogen can be increased and adjusted by methylation to stabilize an SB form.

The exceptional case of arginine, with its extremely basic side chain available for metal-ion coordination, has long been interesting. The cationized molecule was one of the cases carefully studied by the Williams group in their groundbreaking applications of blackbody infrared radiative dissociation (BIRD) to many ion-structure questions including the CS vs SB distinction [81]. These complexes provided an early target for applying IRMPD spectroscopy to this problem using an OPO laser in the hydrogen-stretching region [14], and for application of the free-electron laser in the mid-infrared [20].

2.1.2 Transition Metals

Although transition metal ions are surely not unimportant partners for peptides and enzymes in nature, there is little to report of spectroscopic study of their amino acid interactions. As noted in Table 1, Ag^+ is the only one with a noticeable body of spectroscopic data for monomeric amino acid complexes. For comparison's sake, the comprehensive computational surveys of Mn^{2+} by the Ohanessian group [52, 53] and of Ag^+ by the York group [66] are displayed to fill some gaps in Table 1. Besides the entries in the table, we can note that the spectroscopy of Cd^{2+}His (CS tridentate) was reported [69], as was a computation [73] of Zn^+ (CS bidentate) and Zn^{2+} (SB) with glycine. Closely related is the spectroscopic characterization of the complex of $CdCl^+$ with histidine [69], where the $CdCl^+$ ion behaves in the same way as a singly-charged transition metal (such as Ag^+), and is chelated in a tridentate T[CO,N,N] complex. From these limited examples, we can conclude that the strong chelating interaction of the transition metal ions with Lewis-basic sites leads to maximally chelated CS structures (except for the exceptional case of Pro) always for the Ag^+ ion, and also for Zn^{2+}, Mn^{2+} and other metal ions complexing amino acids possessing Lewis-basic side-chain heteroatoms. If there is no active side chain and a doubly charged transition metal ion, it looks as if salt-bridge stabilization (SB) outweighs solvation interactions (CS), leading to ground state zwitterions for these transition metal ions with aliphatic amino acid ligands. Thus, for the example of Mn^{2+} at least, SB is predicted to be the favored ground state for the aliphatic amino acids. The transition metal ions considered here all have a filled (Ag^+, Zn^{2+}, Cd^{2+}) or half-filled (Mn^{2+}) *d*-shell, making their interactions relatively uncomplicated. Consideration of partially filled shells, giving the complications of non-zero spin and non-spherical electron distributions, is for the future.

2.1.3 Deprotonated Ligands

For doubly charged cations, the possibility is opened up of complexation of the metal ion with a deprotonated amino acid ligand, $[M^{2+}(AA\text{-}H)^-]^+$. It seems that it may actually be easier to produce these deprotonated complexes from an electrospray source than the intact $[M^{2+}(AA)]^{2+}$ complexes for transition metal ions, and reports about such complexes are appearing. The most straightforward outcome is for the metal ion to be simply chelated by the anionic ligand in the same pattern as the corresponding non-deprotonated complex. In these cases, the ligand is deprotonated to give the expected carboxylate anion, which then chelates to give an $[M^{2+}(AA\text{-}H)^-]^+$ tridentate complex T[CO^-,N,X], or, in the case of lysine at least, a bidentate complex B[CO_2^-,N]. This pattern seems natural for a strongly Lewis-basic side-chain group combined with a strongly interacting transition metal ion. The cases of $[Zn^{2+}(His\text{-}H)^-]^+$ [69], $[Cd^{2+}(His\text{-}H)^-]^+$ [69], $[Pb^{2+}(Phe\text{-}H)^-]^+$ [82], and $[Pb^{2+}(Lys\text{-}H)^-]^+$ [83] were all shown spectroscopically to follow this pattern. In a slight variation of this theme in the $[Pb^{2+}(Glu\text{-}H)^-]^+$ complex, the site of deprotonation is still carboxyl, but it is the side-chain COOH which deprotonates giving a tridentate complex which can be described as a T[CO_2^-,N,CO] complex [82].

However, when the Fridgen group looked at Pb^{2+} complexes of the aliphatic amino acids, a different and unexpected pattern of deprotonated complexation was uncovered. Initially working with the complex of Pb^{2+} with deprotonated glycine [84], it was found that, rather than the expected C-terminal carboxyl deprotonation and metal binding by the carboxylate as diagramed in structure-types (ii) and (iii) in Scheme 3, IRMPD spectroscopy in the hydrogen stretching region firmly indicated the N-deprotonated structure of type (i) in Scheme 3. This bidentate conformation might be labeled B[N^-,CO]. Their calculations convincingly supported this as the most stable isomer.

Follow-up experiments [83] showed this same pattern (Scheme 3 structure (i)) for all the aliphatic amino acids (Ala, Val, Leu, Ile, and Pro). This distinctive

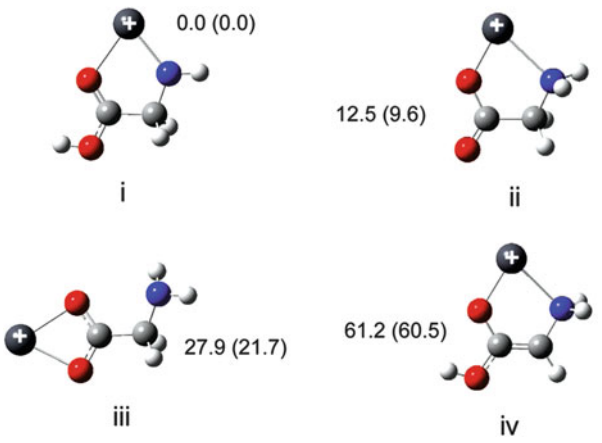

Scheme 3 Possible structures for the deprotonated Pb^{2+} glycine complex. The amine-deprotonated structure (i) is identified spectroscopically as the predominant form for glycine and the other aliphatic amino acids including Pro. Reproduced with permission from [84]

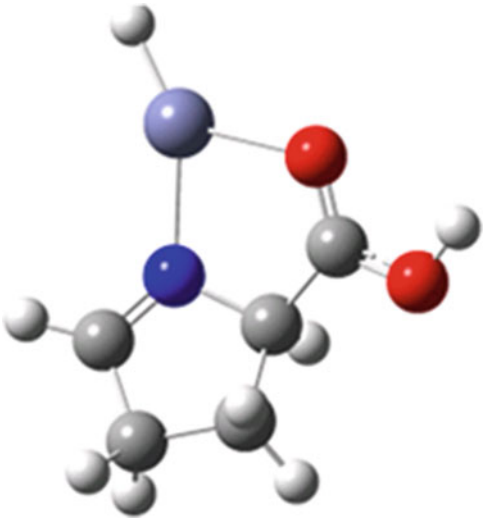

$[Zn^{2+}(Pro\text{-}H)^{-}]^{+}$

Scheme 4 The novel structure of the deprotonated zinc/proline complex. Adapted with permission from [85]

binding of Pb^{2+} to the deprotonated amino nitrogen of the amino acid was rationalized as reflecting a preference by the soft acid Pb^{2+} to bind the soft base NHR^{-} rather than the harder base COO^{-}.

Looking at complexes of the more active zinc ion [85], the proline complex revealed a further variation of this nitrogen/metal-ion binding theme for the deprotonated proline/zinc complex $[Zn^{2+}(Pro\text{-}H)^{-}]^{+}$. This was assigned the interesting structure shown in Scheme 4 having the same N-deprotonated structure as the Pb^{2+} complex, except that a proton has moved from the proline ring to the metal ion (formally an oxidative addition), giving the novel structure shown.

2.1.4 Anionic Complexes

In contrast with the dozens of studies of metal cation complexes with peptides, there have been only a small number of spectroscopic reports on complexes of anions. A study by the Williams group [86] of halide anion complexes with Glu, His, and Arg showed clear cut characteristic IRMPD spectra, indicating CS-type isomers favored for Glu and His, vs SB isomers for Arg (Scheme 5). As could be expected, the halide ion binds differently than metal cations, forming effectively hydrogen bonds to two acidic protons. Spectroscopically speaking, the halide ions give relatively small frequency shifts of the characteristic carbonyl (CS) or carboxylate (SB) stretching frequencies, because the perturbing anion is quite remote and isolated from the region of the CO or COO^{-} normal mode.

The Kass group [87] recently reported the IRMPD spectroscopy and calculations of the Cl^{-} complex of proline in a report reinforcing the cautionary note regarding

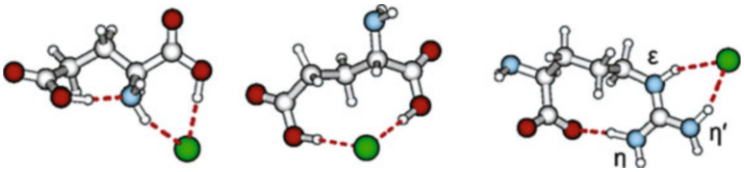

Glu X^- CS Isomers Arg X^- SB Isomer

Scheme 5 Anionic complexes of Glu and Arg amino acids with halide anions. Adapted with permission from [86]

simple but misleading, IRMPD structure results. The spectrum observed strongly indicated a CS conformation for this complex, giving an excellent fit to the calculated spectrum of a CS isomer, which is one of several isomers (both CS and SB) calculated to lie near the lowest energy. However, impelled by the fact that careful calculations indicated a very low-lying SB structure which should be populated, they looked more closely at the dissociation kinetics, finding a deviation from linear logarithmic decay of the parent ion near the point of complete dissociation (>79%). Noting the discussions by Prell et al. [48, 88, 89] of using photokinetic data to sort out misleading IRMPD results for mixed-isomer systems, they considered it most likely that the SB isomer was actually present at about 44% abundance, but was suppressed in the IRMPD spectrum because its dissociation is much slower than that of the strongly observed CS isomer.

2.1.5 Tripositive Complexes

The severe instability of a triply charged metal cation with a ligand as small as a single amino acid has made the production and characterization of such ions elusive. It was thus of considerable interest that a collaboration of York and FELIX groups was able to observe triply charged complexes of La(III) with a protected Trp derivative, with only innocuous modifications separating the complexes studied from the ideal complex of the bare amino acid [90]. The ligand (L) was the end-group derivatized *N*-acetyl-tryptophan-methyl ester. The two complexes for which they achieved IRMPD characterization were the solvent-stabilized $La(III)L(ACN)_2^{3+}$, where ACN is acetonitrile; and the dimer complex $La(III)L_2^{3+}$. In both cases, the IRMPD spectrum gave an excellent fit to a calculated spectrum for a conformation having CS character, and having chelation of the metal ion by all the available Lewis-basic sites for each amino acid ligand, namely the carbonyl oxygen, the amino nitrogen, and the π system of the Trp side chain.

2.1.6 Dimer Complexes

In the domain of ionic complexes, the term "dimer" is usually used for a composite system AXB, where A and B are ligands, which may be the same ("homogeneous" or "symmetric") or different ("heterogeneous" or "asymmetric"), and X is a charged core group, usually a proton or a metal ion. These are often among the most abundant ions in the electrospray or molecular expansion products, and there has been some attention to the structures and spectroscopy of dimers involving peptide-related ligands.

There have been a number of studies of peptide proton-bound dimer spectroscopy in collaborations involving, among others, the Paris groups, the Fridgen group, the McMahon group, and the FELIX group, using the CLIO FEL [91–95], the FELIX FEL [96], and also benchtop OPOs in the H-stretching region [97]. These results are outside our present scope.

For metal-ion dimer complexes with amino acid ligands, it has been interesting to characterize the two ligands with respect to their CS or SB nature. In the mid-infrared this has proved to be difficult. In the case [98] of the $M^{2+}Trp_2$ dimers, where M was Ca, Sr, Ba, Zn, Cd, Mn, Co, and Ni, it was readily established from the mid-IR spectra that all dimers contain at least one CS ligand. Assigning the second ligand was more problematic because of the lack of clear positively diagnostic markers for the SB conformation, but the weight of evidence was for a CS/SB combination in all cases except Ni, which was considered to be CS/CS. A later further study [99] of the Mg, Ca, Sr, and Ba dimers of Trp in the H-stretching region using an OPO laser showed the H-stretching wavelength region (~3,000–4,000 cm^{-1}) to be much more clearly diagnostic, and gave a more definitive assignment of CS/CS for the Sr^{2+} and Ba^{2+} complexes, vs CS/SB for the Mg^{2+} and Ca^{2+} complexes. Finding a bias toward more CS binding specifically in the Ba^{2+} case presented an interesting contrast, in that much previous work with Ba^{2+} monomer complexes had always shown this metal's complexes to be more prone to SB conformations than the smaller alkaline earth metals.

The dimer complexes of histidine with Zn^{2+} and Cd^{2+} were also examined in the mid-IR [69], with a similar outcome to the mid-IR study of the Trp complexes. It was easily established that at least one ligand in each case was CS, and it was considered most likely that at least some of the population had an SB ligand forming CS/SB dimers. However, again the lack of definitive markers for possible SB ligands left uncertainty about the presence and extent of such ligands.

2.2 Small Peptides

2.2.1 CS and SB Binding

Among the earliest FEL work applying IRMPD spectroscopy to ion structures was the spectroscopy at CLIO of protonated dialanine [34]. A close match to the

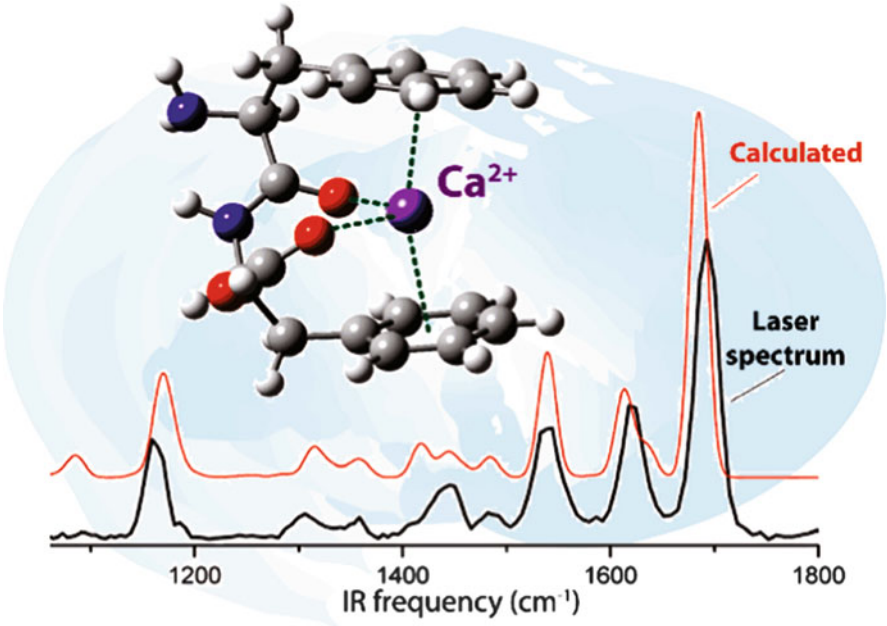

Fig. 4 The caging effect of the strong double cation-π interaction with the doubly charged calcium ion and the PhePhe ligand. Reproduced with permission from [101]

calculated spectrum was obtained, showing definitively that protonation was at the amino nitrogen. On the other hand, a report for protonated AlaHis soon followed [33], showing that in that case the site of protonation was at the imidazole side-chain nitrogen (that nitrogen being more basic than the amino nitrogen).

Further pioneering efforts at CLIO gave spectra for metal ion complexes of small peptides [100], namely the sodium ion complexes of di- and tri-glycines and -alanines. About the same time, the group at FELIX in collaboration with our group reported results for sodium and potassium complexes of PheAla and AlaPhe, giving clear evidence for cation-π coordination of the phenyl ring [12].

The cation-π theme was pursued in studies of the double-π system PhePhe, in which cations, especially the alkaline earths, are encapsulated in compact structures [101], as in Fig. 4. Chelation by both phenyl groups forming a cage in this way is strongly enforced for the doubly charged metal ions. For singly charged counterparts (alkali metals and Ag^+), binding of the N-terminal aromatic ring is still strong, but the cage is more likely to open up by giving up the binding of the C-terminal ring; the spectra of these latter complexes have broader peaks and more congestion, indicating conformational flexibility. The cage-structuring effect of the doubly charged cations is thus enhanced by the stronger micro-solvation experienced by the higher ion charge.

Accumulating experience indicates that salt-bridge formation in metal ion complexes of dipeptides and larger peptides is less common than for the mono-amino

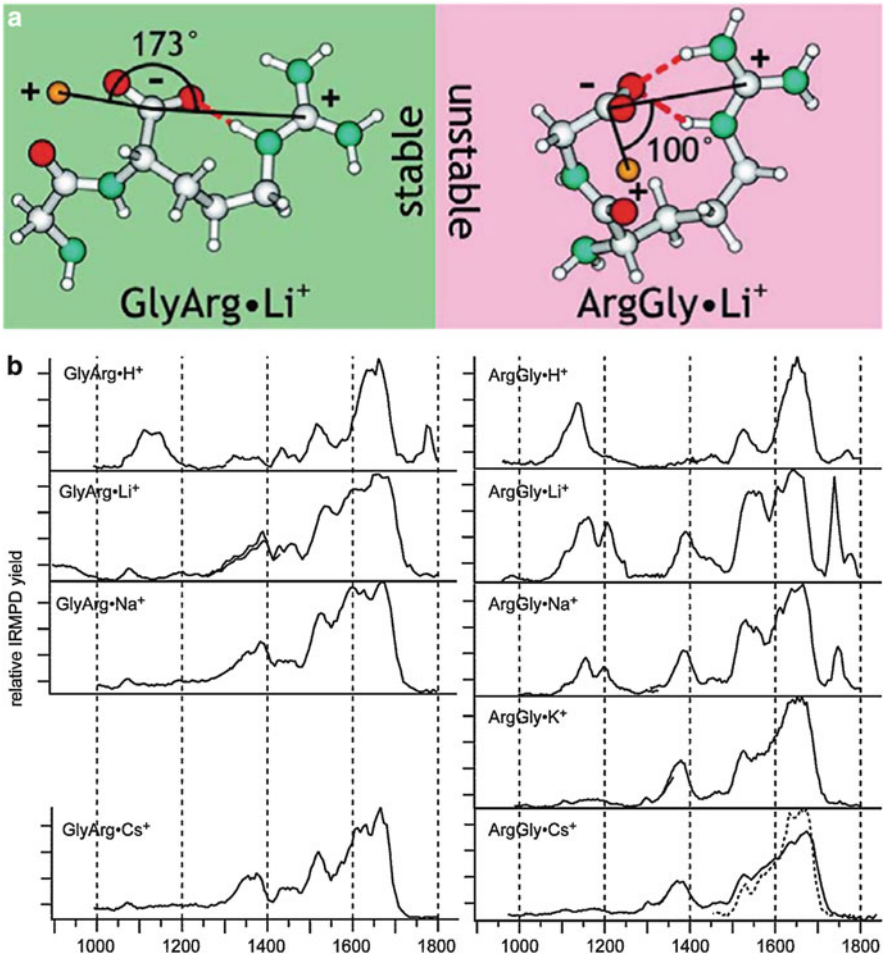

Fig. 5 Sequence dependence of the ability of an alkali cation to stabilize the salt bridge. (**a**) Structures of the most stable zwitterion form for the lithium ion complexes; (**b**) IRMPD spectra of the complexes. Arg at the C-terminus favors salt bridging, while the reverse sequence (in combination with a small ion such as Li^+ or Na^+) can give a stable CS ion as signaled by the strong peak near 1,750 cm^{-1} of the ArgGly complexes of those ions. Reproduced with permission from [102]

acid complexes, and so far all of the ground-state salt-bridge instances which have been characterized spectroscopically have been either singly charged dipeptide complexes containing at least one arginine residue [35, 48, 102] or dipeptide complexes of doubly charged metal ions [79].

Among Arg-containing dipeptides, the work of the Williams group [35, 48, 102] indicates that those with C-terminal Arg are more likely to favor SB formation, with the protonated arginine side chain forming an excellent linear salt bridge in combination with the deprotonated carboxyl and the metal ion (Fig. 5a, left). The salt bridge formed with N-terminal Arg is less favorable (Fig. 5a, right), having a

sharp bend. All the dipeptide/alkali ion complexes reported by Prell et al. [35, 48, 102] with C-terminal Arg form ground-state SB conformations, whereas those with N-terminal Arg do so only for larger alkali metals, Na^+ being the crossover point showing a mixture of SB and CS conformations. A similar theme was reported for protonated dipeptides [35]: the complexes H^+ArgXxx (Xxx being any of various residues) were all CS conformations, but, with an Arg residue at the C-terminus in H^+ArgArg, the conformation was a salt bridge. The spectroscopic evidence for all these cases is displayed in Fig. 5b, with the CS conformations being clearly marked by the strong short-wavelength peak (1,750 cm^{-1}) corresponding to the carboxyl C=O stretch.

The examples just described for Arg-containing dipeptides illustrate the delicate role played by geometric factors in determining the most favorably chelated conformations for wrapping an ion in a peptide ligand. Similarly, sequence dependence was seen for complexes of (Ala,Phe) with Ba^{2+} [79], as shown in Fig. 6. PheAla forms a complex displaying the expected CS absorption peaks, comprising the metal-bound carboxyl carbonyl stretch (in the vicinity of 1,700 cm^{-1}), Amide I (1,620 cm^{-1}) and Amide II (1,540 cm^{-1}), and the free carboxyl COH bend (1,150 cm^{-1}). On the other hand, the AlaPhe complex switches completely, and clearly displays the characteristics of conversion to SB, most notably the appearance of a strong feature around 1,400 cm^{-1}, attributable to NH bending motions of the protonated amine nitrogen, along with apparent disappearance of the free COH bend at 1,150 cm^{-1}. An even subtler geometric distinction was found for the diastereomers of alkali metal complexes of PhePhe, where the DL and LL diastereomers were found to have substantially different conformational preferences [103].

The increasing favorability of the SB conformation for increasingly large doubly charged alkaline earth ions is pointed out in Fig. 7. The spectroscopic evidence is shown for the M^{2+}AlaAla complex, which progresses from mostly CS conformation

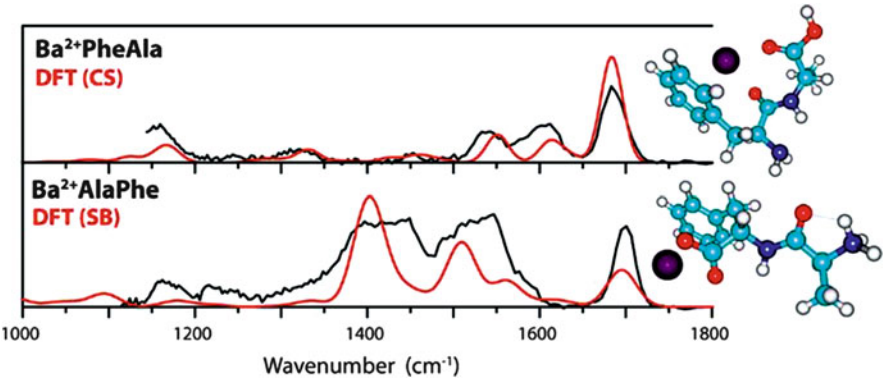

Fig. 6 Influence of sequence on the formation of CS vs SB structures. Complexes of Ba^{2+} with AlaPhe and PheAla are found to behave differently based on the comparison of experimental and theoretical spectra. Reproduced with permission from [79]

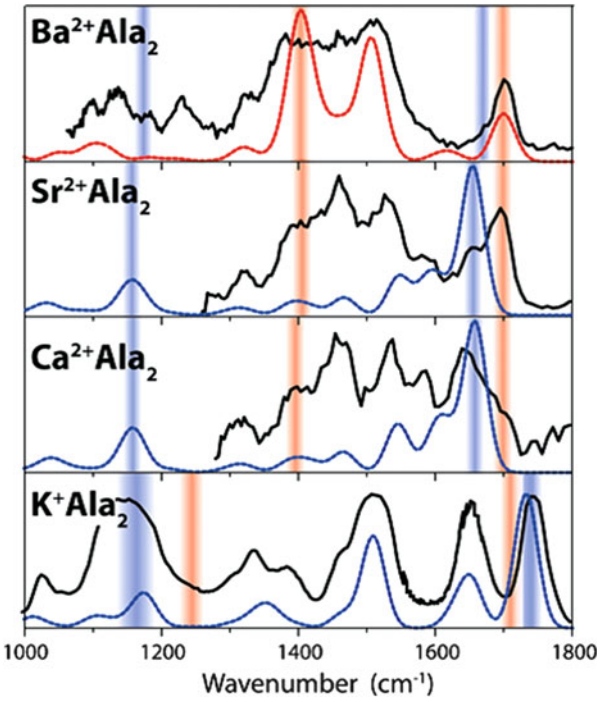

Fig. 7 Series of AlaAla metal ion complex spectra showing the relative prominence of SB vs CS signature features. Calculated positions of the characteristic SB peaks are indicated in *red*, and CS peaks are in *blue*. Traces of calculated spectra show the most stable SB conformation in the Ba complex (*red bars*) and the most stable CS conformations for the Sr, Ca, and K complexes (*blue bars*). Reproduced with permission from [79]

for Ca^{2+}, to mostly SB conformation for Ba^{2+}. The K^+ complex is fully CS, as expected.

Noting the interesting exceptions discussed above (as well as the iminol complexes described in the following section), most dipeptide and all tripeptide and higher complexes that have been characterized spectroscopically possess CS as opposed to SB ground states. Much detail has been obtained regarding the spectroscopic characteristics of CS-bound complexes. Taking trialanine as a typical set of spectra for a ligand without complicating side chains [104], Fig. 8 lays out the four characteristically strong and reliable features common to this spectroscopy. The two normal modes belonging to the COOH C-terminus (CO stretch and COH bend) are still prominent, even though they are outnumbered by the two sets of amide linkage modes (CO stretch, or Amide I, and NH bend, or Amide II). The modes follow very regular wavelength shifts correlated with the relative binding strengths of the series of metal ions. Thus the carboxylic acid CO stretch shows a systematically increasing red shift from 1,790 cm^{-1} in the neutral ligand, down to ~1,690 cm^{-1} for the divalent Ca^{2+} cation. The Amide I band (which, in the same way as the carboxylic acid band, has strong participation of a metal-bound oxygen in the normal mode) shows a similar progressive red shift, from ~1,700 to ~1,600 cm^{-1}. On the other hand, the Amide II band, which primarily involves atoms not directly bound to the metal, shows a progressive but smaller shift in the

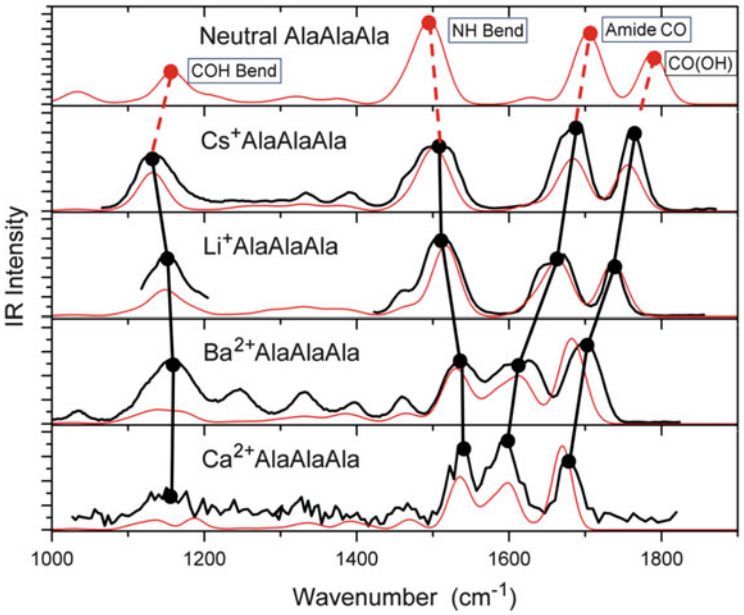

Fig. 8 IRMPD spectra of the trialanine complexes (*black traces*), along with the calculated CS (*red*) conformations considered most likely to dominate the ground state populations. The IRMPD plot for the Na^+ complex was extracted from [100]. Figure reproduced with permission from [104]

blue direction from ~1,500 to ~1,530 cm^{-1}, and the COH bend, also remote from metal-bound atoms, shows no discernible systematic shift.

2.2.2 Iminol Complexes

In nature, as in the model studies discussed thus far, metal ions of the main-group elements form complexes with the peptide backbone by interaction with the amide carbonyl oxygens, along with side-chain chelation sites which may be conformationally available. The Paris group laid out the guiding principle that the metal ion (Na^+) tends to coordinate as many amide carbonyls as possible in glycine peptide chains [105]; this interaction is so strong that it is reasonable to anticipate similar tendencies for more highly decorated chains as well. However, we recognized that peptide binding of highly charged transition metal ions in condensed phases often follows a fundamentally different pattern, primarily binding instead via strong metal bonds to deprotonated amide nitrogens, and such a pattern is possible also for gas-phase model systems involving more active metal ions than alkali metals [106].

For the intact peptide to bind in this way in a (non-deprotonated) gas-phase complex, the deprotonation of the amide nitrogen must transfer the proton to another site. In cases reported so far, this has meant tautomerism of the amide

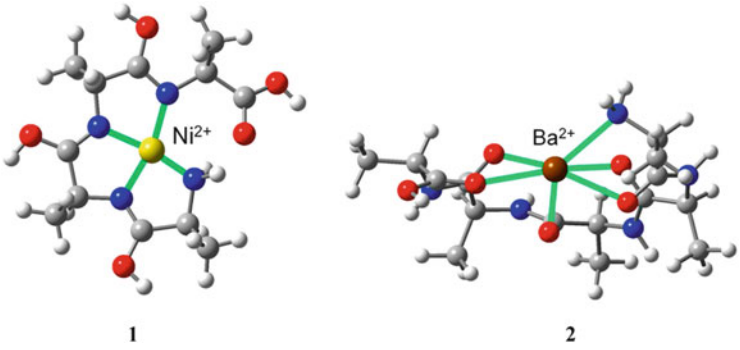

Scheme 6 Lowest-energy structures for complexes of Ni^{2+} and Ba^{2+} with poly-alanines. Formation of an iminol structure is observed for the Ni^{2+} complex. Reproduced with permission from [107]

linkage into the imine enol, or *iminol*, tautomer, analogous to an enol. Scheme 6 illustrates this theme by comparing a highly chelated barium ion having multiple carbonyl oxygen ligands [108], with a transition metal ion Ni^{2+} chelated by three amide nitrogens, each in the iminol configuration, along with the fourth nitrogen from the N-terminus (computed structure for $Ni^{2+}(Ala)_4$ shown for illustration) [107].

Solid spectroscopic evidence for iminol ground states (with computational support) was reported for several complexes of PhePhe [109]. As displayed in Fig. 9, iminol binding is preferred for Co^{2+}, Ni^{2+} and Mg^{2+}, while Ca^{2+} and Li^{+} prefer CS binding. The tendency toward iminol binding appears to correlate with overall binding energy, so that the strongly binding Mg^{2+}, Ni^{2+}, and Co^{2+} ions clearly match the expected iminol spectral patterns, while the more weakly binding K^{+} and Ca^{2+} ions show the familiar pattern of CS binding (as exemplified in Fig. 8).

A subsequent survey of HisGly complexes with most of these same metal ions gave similar results [110]. The strong-binding ions Mg^{2+} and Ni^{2+} gave clear spectra for iminol, while the weaker-binding ions K^{+}, Ca^{2+}, and Ba^{2+} gave CS spectra. Looking at larger peptides, a more extensive survey was reported with the aim of defining more broadly the scope of the iminol binding theme for gas-phase complexes [107]. Figure 10 compiles the results. A powerful discriminant between iminol and CS conformations was found to be the presence or absence of the Amide II band, which is consistently strong at 1,500–1,550 cm^{-1} for CS (and SB) conformations, but absent for the iminol forms. Unfortunately, no positive marker for the iminol form stands out in this mid-infrared wavelength span, so the presence of a weak but not vanishing band at the Amide II position can only be taken as an indication, but not a proof, that some of the population has taken the iminol form. Results are collected in the figure for six different peptides ranging from two to four residues (considering PheAla and PheGly to be equivalent). For the most part, the patterns described above were confirmed and strengthened, with weakly binding metals K^{+} and Ba^{2+} being clearly CS or SB, and strongly binding Ni^{2+} being equally

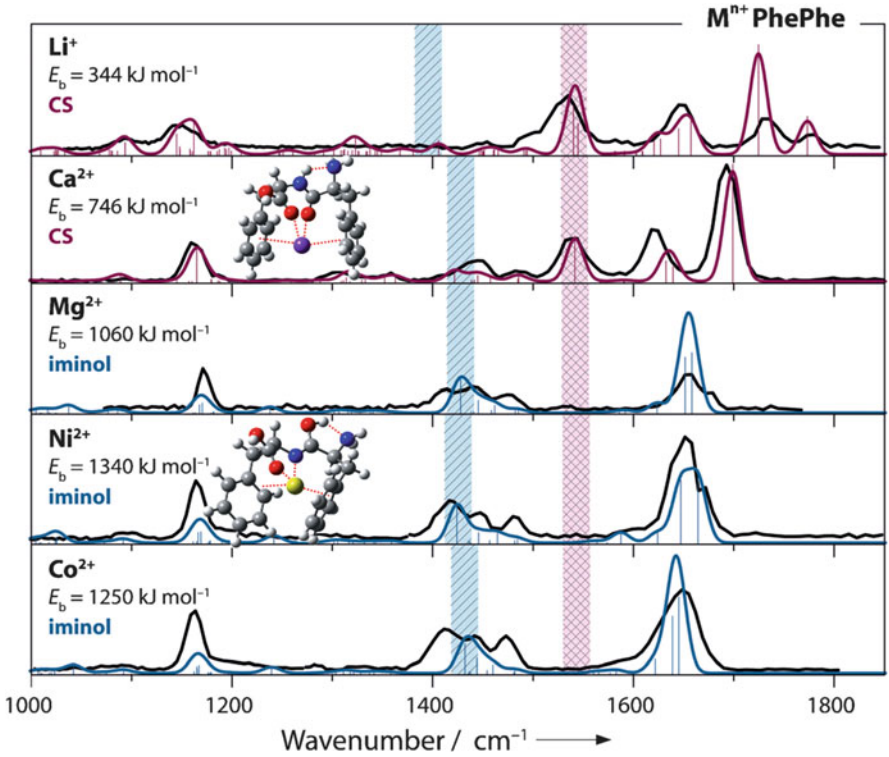

Fig. 9 IRMPD spectra (*black*) compared with calculated CS spectra (*red*) and calculated Iminol spectra (*blue*) for several M^{n+}PhePhe complexes. The *red bar* marks the expected position of the Amide II peak of the CS complex, while the *blue bar* marks that of the iminol COH bending mode. Reproduced with permission from [109]

clearly iminol. However, both Ca^{2+} and Mg^{2+} give indications of being transitional. The Ca^{2+} complexes of the two least strongly chelating ligands, AlaAla and PheAla (or PheGly), appear to have a relatively weak Amide II bands, suggesting partial iminol character, but become positively iminol in appearance for the more effective solvating ligands AlaAlaAla, PhePhe, PheGlyGly, and PheGlyGlyPhe. The Mg^{2+} complexes look positively iminol in character for the weakly solvating dipeptide ligands, but switch to an obvious CS character with the larger PheGlyGly and PheGlyGlyPhe ligands (which presumably give greater microsolvation of the metal ion in favor of CS). It looks as if both these latter metals are close to the point of transition between iminol and CS character, and tend to move to CS predominance as the ligand takes on a greater degree of micro-solvating capacity. The Mg^{2+} (and perhaps Ca^{2+}) results indicating iminol conformations are particularly interesting, because in condensed phase these ions are considered as strongly favoring CS-type coordination to amide CO oxygens [111, 112], while transition metal ions such as Ni^{2+} consistently favor deprotonated amide nitrogen binding (frequently square planar) [113–115].

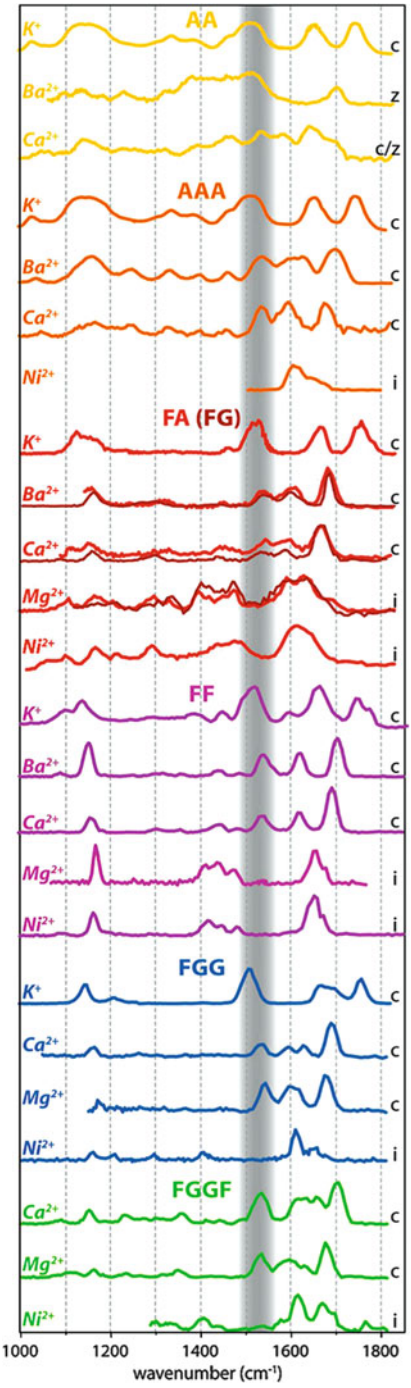

Fig. 10 IRMPD spectra of five metal ions complexed to various peptide ligands (identified by their one-letter amino acid codes). The spectra are grouped by ligand. The *gray shading* indicates the approximate position of the amide NH bending mode (Amide II mode). The presence of this band indicates that the ligand is in the 'normal' amide configuration, while absence of the band suggests a tautomerization to the iminol motif, in which the proton has moved from the amide nitrogen to the amide oxygen atom. The c, z,i-letter code to the right of each spectrum indicates our assignment as charge-solvated, **z**witterion or **i**minol, respectively. Note that the spectra for the FG (PheGly) ligand have been superimposed on the FA (PheAla) spectra in a *slightly darker color*, and that the spectra of this pair of ligands are consistently very similar. Reproduced with permission from [107]

2.3 Infrared: Larger Peptides and Proteins

IRMPD spectroscopy has shown itself to be well suited to pointing up a number of structural themes and transitions as one moves upward from amino acids, through di- and tri-peptides, to larger systems. An overview was offered in our Introduction by the correlation of the three gas-phase spectra juxtaposed in Fig. 1.

Moving out towards longer *n*-residue oligopeptides, a threshold is crossed between about $n = 4$ and $n = 6$, where it becomes no longer favorable to wrap the oligopeptide around a metal ion in a tightly chelated fashion with all carbonyl oxygens and the amine nitrogen coordinated (see Scheme 6, structure 2). The significance of this boundary as a function of different metal ions was explored by our group for $n = 5$ (specifically, for pentaalanine) [116] and by the Ohanessian group, whose studies of Na^+ complexes of Gly_n span this range of ligand sizes [105]. Useful spectroscopic markers of this size transition were identified in the mid-IR spectral region. We found that the tightly chelated class of complexes exhibits spectroscopic characteristics of a terminal COOH which is not perturbed by intramolecular H-bonding. Some or all of these features were prominent for smaller sodium ion complexes of Gly_n ($n \leq 5$) [105] and for the Ca^{2+} and Ba^{2+} complexes of Ala_5 [116]. (It can be seen in the $Ba^{2+}Ala_5$ structure shown in Scheme 6, structure 2, that the tightly wrapped chelation geometry of this complex allows no freedom for H-bonding of the COOH group.) On the other hand, larger alkali ion complexes show spectroscopic characteristics more indicative of a predominantly H-bonded carboxyl group, as expected when there is a surplus of Lewis-basic chelation sites exceeding the chelation-available space around the metal ion.

The Ohanessian group has led a systematic effort to apply spectroscopy and computation to complexes of sodium-complexed peptides, extending to larger sizes with six or more residues [100, 105, 117–119]. Calculations become challenging, and the conformation space becomes enormous, but they have discerned some key structural features from the spectra. Once there are metal-free carbonyl oxygens available, networks of hydrogen bonds can form, and it makes sense to organize the structural possibilities in terms of secondary peptide structures such as helices, sheets, and so on. Of recent interest is the study of the globular-to-helix transition for Na^+Ala_n, where *n* ranges from 8 to 12 [119]. For all peptide lengths, all levels of calculation predict a helical form as the lowest energy, but globular forms are not unreasonably high in free energy. Figure 11 displays the calculated low-energy structures for $n = 8$ for both helical and globular forms. The IRMPD spectra, while not giving very exact agreement with calculated spectra, are able to show that both helical and globular conformations contribute to the observed spectrum at $n = 8$. The IRMPD spectra are interpreted as indicating helical structures for $n = 9$ to 12, with the possibility of some globular contribution for $n = 9$.

The decapeptide gramicidin S has been a target of room temperature IRMPD [120], cold-ion IR/UV [121, 122], and computational [32] spectroscopic studies.

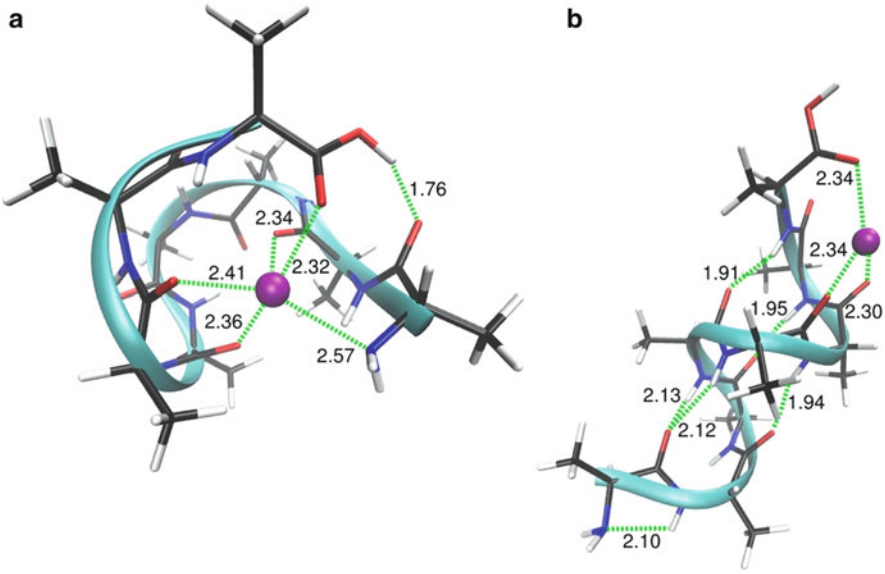

Fig. 11 Na^+Ala_8: (**a**) lowest energy globular structure; (**b**) α-helical structure (lowest energy). Calculations were performed at the M06/6-311+g(d,p)//M06/6-31g(*d*,*p*) level of theory. Reproduced with permission from [119]

Since the most incisive results have come from the cold-ion work, reports on progress there are appropriate to the Rizzo chapter [40].

2.4 Solvation Effects

The thermodynamically driven transition from solution-phase zwitterion ground states to gas-phase canonical tautomers can be probed by progressively adding water molecules to the bare gas-phase complex and characterizing the structure of the resulting complex. In their study of Li^+ and Na^+ complexes with Arg, Bush et al. [123] clearly stated the general principle at work in such progressive hydration studies: "Hydration of the metal ion in these clusters weakens the interactions between the metal ion and the amino acid, whereas hydrogen-bond strengths are largely unaffected. Thus, hydration preferentially stabilizes the zwitterionic structures, all of which contain strong hydrogen bonds." In this particular study, the transition from CS to SB for lithiated Arg was induced by attaching a single water molecule.

Spectroscopy in the hydrogen-stretching region was applied to characterize proton and lithium-ion complexed valine complexes as a function of hydration with up to four water molecules [22]. Although calculations and prior study by black-body infrared dissociation had suggested the possibility of zwitterions,

Kamariotis et al. observed no sign of conversion from CS to SB with up to four waters in either case. The only structural change observed was a switch from CS B [CO,N] to CS C[CO] upon addition of the third water to the lithiated complex.

Fridgen's group has uncovered several structural variations in their spectroscopic study of the formally mono-hydrated complexes of deprotonated amino acids, paralleling their work described above on the corresponding deprotonated bare transition metal complexes. Simplest are the structures where the bare deprotonated complex (see Sect. 2.1.3) is hydrated on the metal ion, without rearrangement. Such a pattern is assigned for the $[Pb^{2+}(Phe\text{-}H)^{-}H_2O]^{+}$ case [82], and for part of the population of the $[Pb^{2+}(Glu\text{-}H)^{-}H_2O]^{+}$ complex (with the ligand deprotonation actually coming off of the side-chain carboxyl) [82]. Also assigned for part of the $[Pb^{2+}(Glu\text{-}H)^{-}H_2O]^{+}$ population are several low-lying variant conformations where the complex switches to a carboxylate zwitterion, while the water molecule remains attached to the metal ion [82].

The aliphatic amino acids present more complicated structure changes upon hydration of the deprotonated complexes. $[Pb^{2+}(Pro\text{-}H)^{-}H_2O]^{+}$ is assigned a carboxylate structure with a proton transferred from the water, which can be viewed as a PbOH+ complexed to a Pro carboxylate zwitterion (Scheme 7a) [83]. For the hydrated Pb^{2+} complexes of the other aliphatic amino acids (Ala, Val, Leu, and Ileu), it was suggested that a structure type with intact carboxylate was most consistent with experiment, although not the lowest in energy. They suggest the structure shown in Scheme 7b, which, interestingly, amounts to a $PbOH^{+}$ cation complexed with the intact (un-deprotonated) amino acid [83].

The more active transition metal Zn^{2+} again differs from Pb^{2+} as in Sect. 2.1, again preferring a structure having a hydrogen atom covalently attached to the zinc atom. $[Zn^{2+}(Pro\text{-}H)^{-}H_2O]^{+}$ (the hydrated zinc-proline counterpart to the lead-proline complex) was assigned as the structure shown in Scheme 7c, which is the structure assigned in Scheme 4 with water attached to the metal ion [85].

Since the aqueous solution-phase structure of amino acids and peptides is normally zwitterionic, while that in the gas phase is frequently non-charge-separated, there is considerable interest in whether, and how completely, the complexes

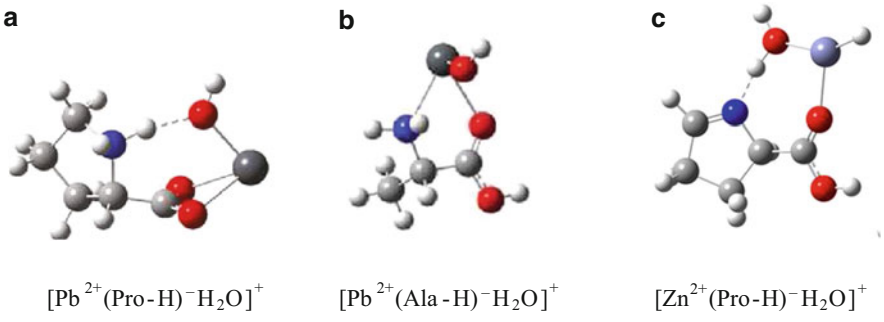

Scheme 7 Assigned structures for the observed hydrated deprotonated M^{2+} alanine complexes. (**a**) Pb^{2+} proline. (**b**) Pb^{2+} with aliphatic amino acids other than proline. (**c**) Zn^{2+} proline. Adapted from [83, 85]

of interest here re-equilibrate to the global minimum structure (more generally to the gas-phase equilibrium mixture of conformations) upon transfer by electrospray to the gas phase. For lack of better information, most spectroscopic studies have tacitly assumed that the structure mix characterized by gas-phase IRMPD represents an equilibrated population. A large number of the studies give this assumption indirect support, in that they show a gas-phase population mixture which is consistent with the best estimates available from computations of the relative free energies and the corresponding thermodynamically equilibrated populations in the gas phase. Concern about whether the gas-phase determinations actually reflect population equilibration is always lurking in the background of presentations of gas-phase experimental results of mixed populations, and there are in fact a number of reports of disagreement with the assumption of equilibration. For example, studies by the Kass group and others (both spectroscopic [124] and non-spectroscopic [87, 125, 126]) of the protonation site of electrosprayed *p*-aminobenzoic acid [124] and the deprotonation sites of tyrosine and *p*-hydroxybenzoic acid [127, 128] showed that the ratio of competing sites can be strongly affected by whether the electrospray is carried out using a protic or a non-protic solvent as well as other variables of the solution. A similar conclusion was affirmed in a following report by Steill and Oomens [129] for deprotonated *p*-hydroxybenzoic acid, where they used mid-infrared IRMPD spectra to show clearly that the site of deprotonation was the carboxyl for protic solvents, and the hydroxyl for aprotic solvents. Thus, the structure of the solution-phase ion was shown to be retained upon transfer to the gas phase. A CID study [130] showed differing fragmentation patterns of ions $[Gly\text{-}H+Zn]^+$, $[Asn\text{-}H+Zn]^+$, and $[Asp\text{-}H+Zn]^+$ from different solvents, which were attributed to structurally differing ion structures formed in the desolvation step, but these conclusions have not yet been confirmed by spectroscopic study.

The Williams group has been interested in the site of attachment of the initial water molecules during progressive solvation of peptides. IRMPD spectroscopy is well suited to characterizing these choices, which are likely to be closely balanced. For instance, at low temperature, the first water attachment to protonated proline is enthalpy controlled at the C-terminus, while at higher temperature the higher entropy of the N-terminal site induces a switch to water attachment there [88].

In an experiment of high technical sophistication and promise for the future, the Dopfer group has described the application of a transient three-color UV/UV/IR ion dip technique, which achieves the observation of the IR action spectrum with a time resolution of a few picoseconds after ion formation. A recent application [131] was to the mono-hydrated cation of acetanilide ($AA^+ \cdot H_2O$), which provides a model for a hydrated peptide amide linkage. As shown in Fig. 12, the ion is initially hydrated at the CO, but the water molecule migrates around to the NH site. The figure displays the time sequence of the evolution from the reactant IR spectrum to the product IR spectrum, revealing a time scale of about 5 ps for this reaction (at the cryogenic temperature of the supersonic beam expansion used to generate the original hydrated molecules).

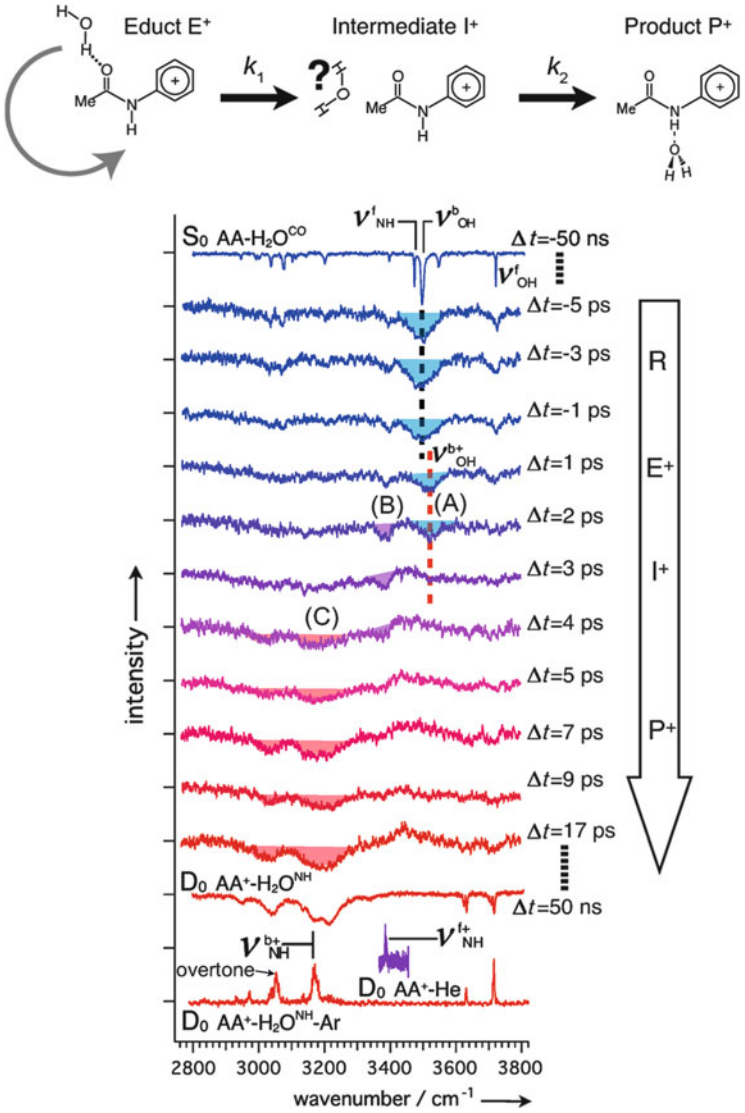

Fig. 12 Time-resolved IR dip spectra of acetanilide$^+$-H_2O. The spectra at $\Delta t = -50$ ns and 50 ns are "static" IR spectra of the CO-bound and NH-bound isomers in the neutral and cationic states measured by nanosecond lasers. The IR spectra of cold AA^+-He and AA^+-H_2O-Ar clusters generated by electron impact ionization are also shown for comparison. Reproduced with permission from [131]

3 Visible/UV and Electronic Spectroscopy

Compared with the recent ferment of activity in the infrared spectroscopy of ions, attention to the UV/visible spectroscopic region has been less active. Among the reasons for this lower interest are, first, the low information content of the typical (room temperature) spectra of molecules of chemical interest, which characteristically show a small number of broad peaks and shoulders, in which a few individual peaks occupy a substantial fraction of the total useful wavelength range, and, second, the greater difficulty and lower confidence of the calculations (most often time-dependent density functional theory (TDDFT) for systems large enough to be interesting) of electronic transitions compared with the high precision and confidence which has evolved for properly scaled vibrational calculations (both ab initio and DFT). It has up to now been unusual for interesting structural questions about larger ions to be answered definitively by correlation of UV/vis action spectra with quantum-chemical calculations.

Although considerations such as these have led to a less active field of UV/visible spectroscopic study compared with infrared study, this wavelength region offers some unique advantages, particularly for studies oriented toward kinetics, dynamics, thermodynamics, and mechanisms of gas-phase ion chemistry. As a particular example, we can mention the ability to initiate a chemical process with the insertion of a very accurately known (single-photon) increment of several eV of internal energy at a precisely determined time (for a view of some of these possibilities, see, for instance, [132]). Control of photon polarization is possible [133]. Moreover, excited electronic reaction and dissociation pathways, often involving radical ion chemistry, can be accessed in this way, which is not possible with vibrational activation.

A leading group in the exploration of the capabilities and limitations of UV/vis spectroscopy of metal complexes is the Nottingham group (Stace et al.), which has pioneered the use of novel ion-source technologies to produce interesting complexes for action-spectroscopic study. They reviewed the field in 2010 [6].

The Lyon group has, within the last few years, greatly expanded the UV/vis spectroscopy of bio-relevant ions (for example), including some metal-cationized peptides and proteins [134]. A thoroughly analyzed case [135] of a UV spectrum of a peptide system is the observation and comparison of the AcGlyGlyGlyTrpNH$_2$Ag$^+$ and AcHisGlyGlyGlyTrpNH$_2$Ag$^+$ complexes, which serve as models for the interesting prion octarepeat system (Fig. 13). The spectra have broad peaks with low information content, and it is hard to separate the features reflecting charge transfer vs intrachromophore transitions within the indole moiety of Trp. However, a distinctive influence of the introduction of His is observed in the form of a shift and enhancement of a feature at 280 nm in the latter peptide, and the authors analyze this peak as showing a close interaction of the imidazole lone-pair nitrogen of the His residue with the silver ion, along with cation-π binding to the indole ring of Trp. This wide-ranging study of the metal binding site in the prion octarepeat neighborhood also included ion mobility, IRMPD spectroscopy in the

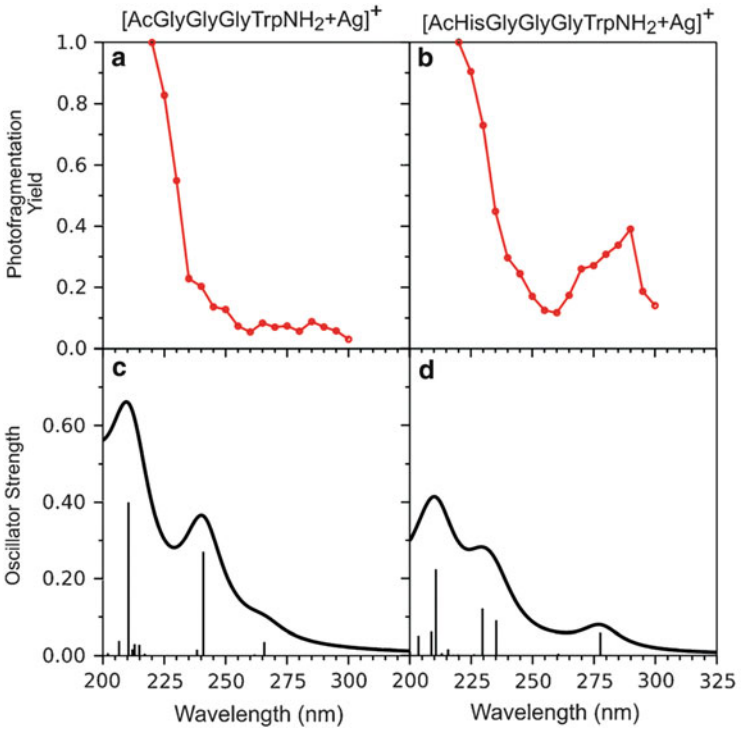

Fig. 13 Experimental photodissociation yield (*red*, arbitrary units) and calculated UV absorption spectra (*black*) for $[AcGlyGlyGlyTrpNH_2 + Ag]^+$ (**a**, **b**) and $[AcHisGlyGlyGlyTrpNH_2 + Ag]^+$ (**c**, **d**). Reproduced with permission from [135]

H-stretching region, and computations, so their conclusions were more broadly based than the UV spectrum alone would justify.

An illustration of the spectroscopic emergence of a strong isolated chromophore within the interior of a substantially large protein is given by this group's spectroscopy of the cytochrome-c system. The Soret band near 410 nm is nicely observed in the $[M\text{-}6H]^{6-}$ electron photodetachment action spectrum for cytochrome-c, containing the Fe(III) heme chromophore [136] (Fig. 14). The gas-phase peak is very close to the position observed in solution, suggesting that the chromophore is well shielded from solvent interactions in solution.

The UV spectroscopy of anions is apt to become complicated because of the competing possibilities of electron photodetachment and photodissociation as exit channels for the photoexcited anion. A case showing progress in sorting out such complexities was shown by the Lyon group. Complexes $[GSH + M - 2H]^-$ (where M is Ag or Au and GSH is the gamma tripeptide glutathione) were found to give a varying mix of detachment and dissociation at UV wavelengths [137]. The action spectra showed some intensity and structure at wavelengths below 300 nm. Time-dependent density functional theory (TDDFT) calculations gave general accord

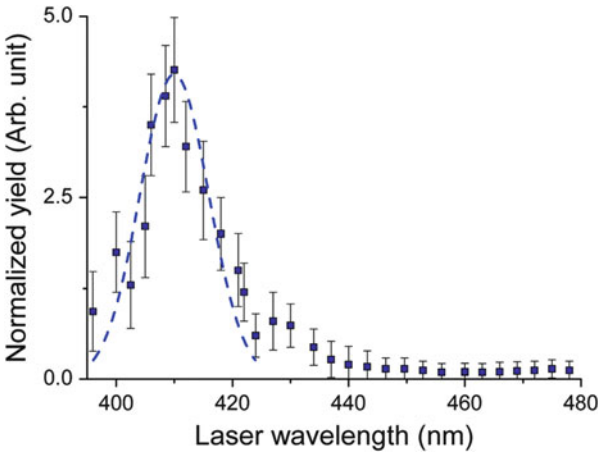

Fig. 14 Laser-normalized electron photodetachment yield measured as a function of the laser wavelength for $[Prot - 6H]^{6-}$, where Prot is cytochrome-c. Reproduced with permission from [136]

with the observed action spectra, and were useful in their interpretation. However, this work was not primarily a spectroscopy exercise, since structure assignments (predicting two-coordinate O-M-S metal binding) were made based on DFT structure calculations, not notably aided by the UV/vis spectra.

UV/vis spectra of silver and gold complexes with tryptophan both show strikingly strong long wavelength peaks at 330 nm for $AgTrp^+$ [74] and 400 nm for $AuTrp^+$ [138]. The peaks are attributed to indole-metal charge transfer, with the metal bound in a charge-solvated fashion to the six-membered ring of the indole group and the amino nitrogen.

Both IR and UV/vis action spectra were used [139] to characterize the radical cations of Trp-containing peptides, in particular $AcGly_3TrpNH_2$. Both types of spectra indicated a canonical π-radical cation structure, ruling out the possibilities of forming a zwitterion, or of an ionization site other than the indole π-system. The spectra are shown in Fig. 15 (compared with the IR spectrum of the protonated peptide). These spectroscopic probes are seen in general as useful structural diagnostics for ionized peptides containing a Trp residue.

The Lyon group made a comparison of the nonapeptide oxytocin (CysTyrIleGlnAsnCysProLeuGly-NH_2) complexed with Cu^{2+}, vs complexation with two protons, and also vs protonated tyrosine [140]. The action spectra in all three cases were considered to be dominated by the tyrosine chromophore, with only weak perturbations among its three environments. The spectroscopic evidence here is not very incisive, although, as Fig. 16 shows, copper complexation resulted in a substantial change in the UV spectrum. This, along with ion mobility and computational evidence, led to the main structural conclusion that the tyrosine side chain did not interact closely with the metal in the Cu(II) complex, while a major structural change was induced by 4-N chelation of the metal ion. The corresponding dianionic complex $[OT - 4H + Cu]^{2-}$ was also studied by photodetachment action spectroscopy [141]. Again, the spectroscopic evidence was not strong, but the arguments pointed toward a structure with copper bound to four deprotonated

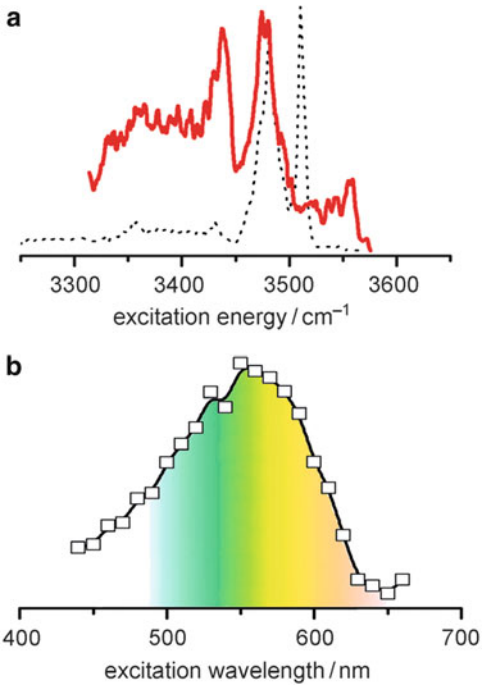

Fig. 15 (**a**) IRMPD spectra of $AcGly_3TrpNH_2^{\bullet+}$ (*solid line*) and $AcGly_3TrpNH_3^{+}$ (*dotted line*). (**b**) Visible photo-fragmentation spectrum of $AcGly_3TrpNH_2^{\bullet+}$. Reproduced with permission from [139]

nitrogens, and the neutral form of the tyrosine side chain. A contrast was drawn with the doubly deprotonated oxytocin ion $[OT\text{-}2H]^{2-}$, in which the tyrosine hydroxyl was considered to be deprotonated.

An interesting approach to probing peptide and protein structures via UV/vis action spectroscopy is the work of the group in Australia using iodotyrosine as a chromophoric label [142], as has been developed by Julian's group at Riverside [143, 144]. The local environment of the tyrosine is sampled by the perturbation of its UV spectrum, with the innocuous iodine substituent atom serving as a one-photon detachable label. The extent of folding to give microsolvation of the tyrosine site is reflected in coalescence of a split feature in the 290 nm region.

Turning to the extreme ultraviolet wavelengths now accessible with synchrotron light sources, VUV spectroscopy of metal complexed polysaccharide ions (photon energies ~8–20 eV) has not yet received much attention, but recent work at the high-energy photon source SOLEIL [145] on polysaccharides is suggestive for the future. In contrast to anionic species, where electron detachment is the primary decomposition pathway, the sodiated species show intense loss of the sodium ion. Attention has been mostly directed to differences in fragmentation patterns among different isomers, but the VUV spectrum of sodiated maltohexose, for example, shows interesting structure with several peaks between 12 and 18 eV, which suggest interesting future possibilities for useful spectroscopic structural information.

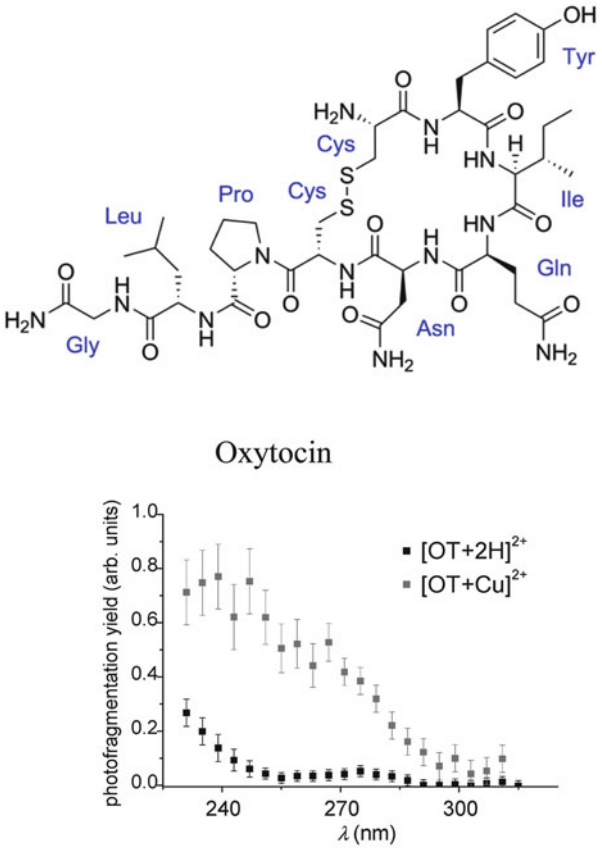

Fig. 16 Experimental fragmentation yields of $[OT + 2H]^{2+}$ and $[OT + Cu]^{2+}$ ions measured as a function of the laser wavelength. Reproduced with permission from [140]

Acknowledgments This work was financially supported by the "Nederlandse Organisatie voor Wetenschappelijk Onderzoek" (NWO). R.C.D. acknowledges support from the National Science Foundation, Grant PIRE-0730072, and expresses gratitude to the FELIX facility for its continuing welcome. The FELIX staff, and particularly Dr. Lex van der Meer and Dr. Britta Redlich, are gratefully acknowledged for their assistance. We thank SURFsara Computing and Networking Services (www.surfsara.nl) for their support in using the Lisa Computer Cluster.

References

1. Rijs AM, Oomens J (2015) IR spectroscopic techniques to study isolated biomolecules. Top Curr Chem. doi:10.1007/128_2014_621
2. MacAleese L, Maître P (2007) Infrared spectroscopy of organometallic ions in the gas phase: from model to real world complexes. Mass Spectrom Rev 26:583–605
3. Eyler JR (2009) Infrared multiple photon dissociation spectroscopy of ions in Penning traps. Mass Spectrom Rev 28:448–467

4. Fridgen TD (2009) Infrared consequence spectroscopy of gaseous protonated and metal ion cationized complexes. Mass Spectrom Rev 28:586–607
5. Polfer NC, Oomens J (2009) Vibrational spectroscopy of bare and solvated ionic complexes of biological relevance. Mass Spectrom Rev 28:468–494
6. Cox H, Stace AJ (2010) Recent advances in the visible and UV spectroscopy of metal dication complexes. Int Rev Phys Chem 29:555–588
7. Burt MB, Fridgen TD (2012) Structures and physical properties of gaseous metal cationized biological ions. Eur J Mass Spectrom 18:235–250
8. Oomens J, Sartakov BG, Meijer G, Von Helden G (2006) Gas-phase infrared multiple photon dissociation spectroscopy of mass-selected molecular ions. Int J Mass Spectrom 254:1–19
9. Wu RH, McMahon TB (2009) Structures, energetics, and dynamics of gas-phase ions studied by FTICR and HPMS. Mass Spectrom Rev 28:546–585
10. Polfer NC, Paizs B, Snoek LC, Compagnon I, Suhai S, Meijer G, von Helden G, Oomens J (2005) Infrared fingerprint spectroscopy and theoretical studies of potassium ion tagged amino acids and peptides in the gas phase. J Am Chem Soc 127:8571–8579
11. Dunbar RC, Steill JD, Oomens J (2010) Cationized phenylalanine conformations characterized by IRMPD and computation for singly and doubly charged ions. PCCP 12:13383–13393
12. Polfer NC, Oomens J, Dunbar RC (2008) Alkali metal complexes of the dipeptides PheAla and AlaPhe: IRMPD spectroscopy. ChemPhysChem 9:579–589
13. Oomens J, Polfer N, Moore DT, van der Meer L, Marshall AG, Eyler JR, Meijer G, von Helden G (2005) Charge-state resolved mid infrared spectroscopy of a gas-phase protein. PCCP 7:1345–1348
14. Bush MF, Forbes MW, Jockusch RA, Oomens J, Polfer NC, Saykally RJ, Williams ER (2007) Infrared spectroscopy of cationized lysine and epsilon-N-methyllysine in the gas phase: effects of alkali-metal ion size and proton affinity on zwitterion stability. J Phys Chem A 111:7753–7760
15. Bush MF, O'Brien JT, Prell JS, Saykally RJ, Williams ER (2007) Infrared spectroscopy of cationized arginine in the gas phase: direct evidence for the transition from nonzwitterionic to zwitterionic structure. J Am Chem Soc 129:1612–1622
16. Carl DR, Cooper TE, Oomens J, Steill JD, Armentrout PB (2010) Infrared multiple photon dissociation spectroscopy of cationized methionine: effects of alkali-metal cation size on gas-phase conformation. PCCP 12:3384–3398
17. Citir M, Hinton CS, Oomens J, Steill JD, Armentrout PB (2012) Infrared multiple photon dissociation spectroscopy of protonated histidine and 4-phenyl imidazole. Int J Mass Spectrom 330:6–15
18. Citir M, Stennett EMS, Oomens J, Steill JD, Rodgers MT, Armentrout PB (2010) Infrared multiple photon dissociation spectroscopy of cationized cysteine: effects of metal cation size on gas-phase conformation. Int J Mass Spectrom 297:9–17
19. Correia CF, Balaj PO, Scuderi D, Maître P, Ohanessian G (2008) Vibrational signatures of protonated, phosphorylated amino acids in the gas phase. J Am Chem Soc 130:3359–3370
20. Forbes MW, Bush MF, Polfer NC, Oomens J, Dunbar RC, Williams ER, Jockusch RA (2007) Infrared spectroscopy of arginine cation complexes: direct observation of gas-phase zwitterions. J Phys Chem A 111:11759–11770
21. Heaton AL, Bowman VN, Oomens J, Steill JD, Armentrout PB (2009) Infrared multiple photon dissociation spectroscopy of cationized asparagine: effects of metal cation size on gas-phase conformation. J Phys Chem A 113:5519–5530
22. Kamariotis A, Boyarkin OV, Mercier SR, Beck RD, Bush MF, Williams ER, Rizzo TR (2006) Infrared spectroscopy of hydrated amino acids in the gas phase: protonated and lithiated valine. J Am Chem Soc 128:905–916
23. Mac Aleese L, Simon A, McMahon TB, Ortega JM, Scuderi D, Lemaire J, Maître P (2006) Mid-IR spectroscopy of protonated leucine methyl ester performed with an FTICR or a Paul type ion-trap. Int J Mass Spectrom 249:14–20

24. Maître P, Lemaire J, Scuderi D (2008) Structural characterization under tandem mass spectrometry conditions: infrared spectroscopy of gas phase ions. Phys Scr 78:058111
25. Scuderi D, Bakker JM, Durand S, Maître P, Sharma A, Martens JK, Nicol E, Clavaguera C, Ohanessian G (2011) Structure of singly hydrated, protonated phospho-tyrosine. Int J Mass Spectrom 308:338–347
26. Scuderi D, Correia CF, Balaj OP, Ohanessian G, Lemaire J, Maître P (2009) Structural characterization by IRMPD spectroscopy and DFT calculations of deprotonated phosphorylated amino acids in the gas phase. ChemPhysChem 10:1630–1641
27. Simon A, MacAleese L, Maître P, Lemaire J, McMahon TB (2007) Fingerprint vibrational spectra of protonated methyl esters of amino acids in the gas phase. J Am Chem Soc 129: 2829–2840
28. Talbot FO, Tabarin T, Antoine R, Broyer M, Dugourd P (2005) Photodissociation spectroscopy of trapped protonated tryptophan. J Chem Phys 2005:122
29. Wu RH, McMahon TB (2008) An investigation of protonation sites and conformations of protonated amino acids by IRMPD spectroscopy. ChemPhysChem 9:2826–2835
30. Correia CF, Clavaguera C, Erlekam U, Scuderi D, Ohanessian G (2008) IRMPD spectroscopy of a protonated, phosphorylated dipeptide. ChemPhysChem 9:2564–2573
31. Dunbar RC, Steill JD, Polfer NC, Oomens J (2009) Gas-phase infrared spectroscopy of the protonated dipeptides H^+PheAla and H^+AlaPhe compared to condensed-phase results. Int J Mass Spectrom 283:77–84
32. Joshi K, Semrouni D, Ohanessian G, Clavaguera C (2012) Structures and IR spectra of the gramicidin S peptide: pushing the quest for low-energy conformations. J Phys Chem B 116: 483–490
33. Lucas B, Gregoire G, Lemaire J, Maître P, Glotin F, Schermann JP, Desfrancois C (2005) Infrared multiphoton dissociation spectroscopy of protonated N-acetyl-alanine and alanyl-histidine. Int J Mass Spectrom 243:105–113
34. Lucas B, Gregoire G, Lemaire J, Maître P, Ortega JM, Rupenyan A, Reimann B, Schermann JP, Desfrancois C (2004) Investigation of the protonation site in the dialanine peptide by infrared multiphoton dissociation spectroscopy. PCCP 6:2659–2663
35. Prell JS, O'Brien JT, Steill JD, Oomens J, Williams ER (2009) Structures of protonated dipeptides: the role of arginine in stabilizing salt bridges. J Am Chem Soc 131:11442–11449
36. Wu RH, McMahon TB (2007) Infrared multiple photon dissociation spectroscopy as structural confirmation for GlyGlyGlyH(+) and AlaAlaAlaH(+) in the gas phase. Evidence for amide oxygen as the protonation site. J Am Chem Soc 129:11312
37. Wu RH, McMahon TB (2009) Protonation sites and conformations of peptides of glycine (Gly(1–5)H(+)) by IRMPD spectroscopy. J Phys Chem B 113:8767–8775
38. Kong XL, Tsai IA, Sabu S, Han CC, Lee YT, Chang HC, Tu SY, Kung AH, Wu CC (2006) Progressive stabilization of zwitterionic structures in [H(Ser)(2–8)](+) studied by infrared photodissociation spectroscopy. Angew Chem Int Ed 45:4130–4134
39. Rizzo TR, Stearns JA, Boyarkin OV (2009) Spectroscopic studies of cold, gas-phase biomolecular ions. Int Rev Phys Chem 28:481–515
40. Rizzo TR, Boyarkin OV (2014) Cryogenic methods for the spectroscopy of large, biomolecular ions. Top Curr Chem. doi:10.1007/128_2014_579
41. Iavarone AT, Patriksson A, van der Spoel D, Parks JH (2007) Fluorescence probe of Trp-cage protein conformation in solution and in gas phase. J Am Chem Soc 129:6726–6735
42. Baer T, Dunbar RC (2010) The Asilomar conference on ion spectroscopy, October 16–20, 2009. J Am Soc Mass Spectrom 21:I1–I3
43. Talbot FO, Rullo A, Yao H, Jockusch RA (2010) Fluorescence resonance energy transfer in gaseous, mass-selected polyproline peptides. J Am Chem Soc 132:16156–16164
44. Wyttenbach T, Witt M, Bowers MT (2000) On the stability of amino acid zwitterions in the gas phase: the influence of derivatization, proton affinity, and alkali ion addition. J Am Chem Soc 122:3458–3464

45. Jockusch RA, Lemoff AS, Williams ER (2001) Hydration of valine-cation complexes in the gas phase: on the number of water molecules necessary to form a zwitterion. J Phys Chem A 105:10929–10942
46. Moision RM, Armentrout PB (2002) Experimental and theoretical dissection of sodium cation/glycine interactions. J Phys Chem A 106:10350–10362
47. Kapota C, Lemaire J, Maître P, Ohanessian G (2004) Vibrational signature of charge solvation vs salt bridge isomers of sodiated amino acids in the gas phase. J Am Chem Soc 126:1836–1842
48. Prell JS, Chang TM, Biles JA, Berden G, Oomens J, Williams ER (2011) Isomer population analysis of gaseous ions from infrared multiple photon dissociation kinetics. J Phys Chem A 115:2745–2751
49. Kish MM, Ohanessian G, Wesdemiotis C (2003) The Na+ affinities of alpha-amino acids: side-chain substituent effects. Int J Mass Spectrom 227:509–524
50. Heaton AL, Moision RM, Armentrout PB (2008) Experimental and theoretical studies of sodium cation interactions with the acidic amino acids and their amide derivatives. J Phys Chem A 112:3319–3327
51. Moision RM, Armentrout PB (2006) The special five-membered ring of proline: an experimental and theoretical investigation of alkali metal cation interactions with proline and its four- and six-membered ring analogues. J Phys Chem A 110:3933–3946
52. Khodabandeh MH, Reisi H, Davari MD, Zare K, Zahedi M, Ohanessian G (2013) Interaction modes and absolute affinities of amino acids for Mn^{2+}: a comprehensive picture. ChemPhysChem 14:1733–1745
53. Khodabandeh MH, Reisi H, Zare K, Zahedi M (2012) A theoretical elucidation of coordination properties of histidine and lysine to Mn^{2+}. Int J Mass Spectrom 313:47–57
54. Bush MF, Oomens J, Saykally RJ, Williams ER (2008) Alkali metal ion binding to glutamine and glutamine derivatives investigated by infrared action spectroscopy and theory. J Phys Chem A 112:8578–8584
55. Armentrout PB, Rodgers MT, Oomens J, Steill JD (2008) Infrared multiphoton dissociation spectroscopy of cationized serine: effects of alkali-metal cation size on gas-phase conformation. J Phys Chem A 112:2248–2257
56. Bush MF, Oomens J, Williams ER (2009) Proton affinity and zwitterion stability: new results from infrared spectroscopy and theory of cationized lysine and analogues in the gas phase. J Phys Chem A 113:431–438
57. Citir M, Hinton CS, Oomens J, Steill JD, Armentrout PB (2012) Infrared multiple photon dissociation spectroscopy of cationized histidine: effects of metal cation size on gas-phase conformation. J Phys Chem A 116:1532–1541
58. Dunbar RC, Hopkinson AC, Oomens J, Siu CK, Siu KWM, Steill JD, Verkerk UH, Zhao JF (2009) Conformation switching in gas-phase complexes of histidine with alkaline earth ions. J Phys Chem B 113:10403–10408
59. Rodgers MT, Armentrout PB, Oomens J, Steill JD (2008) Infrared multiphoton dissociation spectroscopy of cationized threonine: effects of alkali-metal cation size on gas-phase conformation. J Phys Chem A 112:2258–2267
60. Polfer NC, Oomens J, Dunbar RC (2006) IRMPD spectroscopy of metal-ion/tryptophan complexes. PCCP 8:2744–2751
61. O'Brien JT, Prell JS, Steill JD, Oomens J, Williams ER (2008) Interactions of mono- and divalent metal ions with aspartic and glutamic acid investigated with IR photodissociation spectroscopy and theory. J Phys Chem A 112:10823–10830
62. Drayss MK, Armentrout PB, Oomens J, Schaefer M (2010) IR spectroscopy of cationized aliphatic amino acids: stability of charge-solvated structure increases with metal cation size. Int J Mass Spectrom 297:18–27
63. Drayss MK, Blunk D, Oomens J, Schafer M (2008) Infrared multiple photon dissociation spectroscopy of potassiated proline. J Phys Chem A 112:11972–11974

64. Bush MF, Oomens J, Saykally RJ, Williams ER (2008) Effects of alkaline earth metal ion complexation on amino acid zwitterion stability: results from infrared action spectroscopy. J Am Chem Soc 130:6463–6471
65. Wang P, Ohanessian G, Wesdemiotis C (2008) The sodium ion affinities of asparagine, glutamine, histidine and arginine. Int J Mass Spectrom 269:34–45
66. Shoeib T, Siu KWM, Hopkinson AC (2002) Silver ion binding energies of amino acids: use of theory to assess the validity of experimental silver ion basicities obtained from the kinetic method. J Phys Chem A 106:6121–6128
67. Moision RM, Armentrout PB (2004) An experimental and theoretical dissection of potassium cation/glycine interactions. PCCP 6:2588–2599
68. Armentrout PB, Chen Y, Rodgers MT (2012) Metal cation dependence of interactions with amino acids: bond energies of Cs + to Gly, Pro, Ser, Thr, and Cys. J Phys Chem A 116: 3989–3999
69. Hofstetter TE, Howder C, Berden G, Oomens J, Armentrout PB (2011) Structural elucidation of biological and toxicological complexes: investigation of monomeric and dimeric complexes of histidine with multiply charged transition metal (Zn and Cd) cations using IR action spectroscopy. J Phys Chem B 115:12648–12661
70. Stearns JA, Mercier S, Seaiby C, Guidi M, Boyarkin OV, Rizzo TR (2007) Conformation-specific spectroscopy and photodissociation of cold, protonated tyrosine and phenylalanine. J Am Chem Soc 129:11814–11820
71. Fleming GJ, McGill PR, Idriss H (2007) Gas phase interaction of L-proline with Be2, Mg2 and Ca2 ions: a computational study. J Phys Org Chem 20:1032–1042
72. Jockusch RA, Lemoff AS, Williams ER (2001) Effect of metal ion and water coordination on the structure of a gas-phase amino acid. J Am Chem Soc 123:12255–12265
73. Ai HQ, Bu YX, Han KL (2003) Glycine-Zn+/Zn2+ and their hydrates: on the number of water molecules necessary to stabilize the switterionic glycine-Zn+/Zn2+ over the nonzwitterionic ones. J Chem Phys 118:10973–10985
74. Antoine R, Tabarin T, Broyer M, Dugourd P, Mitric R, Bonacic-Koutecky V (2006) Optical properties of gas-phase tryptophan-silver cations: charge transfer from the indole ring to the silver atom. ChemPhysChem 7:524–528
75. Strittmatter EF, Lemoff AS, Williams ER (2000) Structure of cationized glycine, gly·M^{2+} (M = Be, Mg, Ca, Sr, Ba), in the gas phase: intrinsic effect of cation size on zwitterion stability. J Phys Chem A 104:9793–9796
76. Hoyau S, Pelicier JP, Rogalewicz F, Hoppilliard Y, Ohanessian G (2001) Complexation of glycine by atomic metal cations in the gas phase. Eur J Mass Spectrom 7:303–311
77. Dunbar RC, Polfer NC, Oomens J (2007) Gas-phase zwitterion stabilization by a metal dication. J Am Chem Soc 129:14562–14563
78. Gronert S, Simpson DC, Conner KM (2009) A reevaluation of computed proton affinities for the common alpha-amino acids. J Am Soc Mass Spectrom 20:2116–2123
79. Dunbar RC, Steill J, Polfer NC, Oomens J (2009) Peptide length, steric effects and ion solvation govern zwitterion stabilization in barium-chelated di- and tripeptides. J Phys Chem B 113:10552–10554
80. Drayss MK, Blunk D, Oomens J, Gao B, Wyttenbach T, Bowers MT, Schafer M (2009) Systematic study of the structures of potassiated tertiary amino acids: salt bridge structures dominate. J Phys Chem A 113:9543–9550
81. Jockusch RA, Price WD, Williams ER (1999) Structure of cationized arginine (Arg center dot M+, M = H, Li, Na, K, Rb, and Cs) in the gas phase: further evidence for zwitterionic arginine. J Phys Chem A 103:9266–9274
82. Burt MB, Fridgen TD (2013) Gas-phase structures of Pb2+−cationized phenylalanine and glutamic acid determined by infrared multiple photon dissociation spectroscopy and computational chemistry. J Phys Chem A 117:1283–1290

83. Burt MB, Decker SGA, Atkins CG, Rowsell M, Peremans A, Fridgen TD (2011) Structures of bare and hydrated [Pb(AminoAcid-H)](+) complexes using infrared multiple photon dissociation spectroscopy. J Phys Chem B 115:11506–11518
84. Atkins CG, Banu L, Rowsell M, Blagojevic V, Bohme DK, Fridgen TD (2009) Structure of [Pb(Gly-H)](+) and the monosolvated water and methanol solvated species by infrared multiple-photon dissociation spectroscopy, energy-resolved collision-induced dissociation, and electronic structure calculations. J Phys Chem B 113:14457–14464
85. Gholami A, Fridgen TD (2013) Structures and unimolecular reactivity of gas-phase [Zn(Proline-H)](+) and [Zn(Proline-H)(H_2O)](+). J Phys Chem B 117:8447–8456
86. O'Brien JT, Prell JS, Berden G, Oomens J, Williams ER (2010) Effects of anions on the zwitterion stability of Glu, His and Arg investigated by IRMPD spectroscopy and theory. Int J Mass Spectrom 297:116–123
87. Schmidt J, Kass SR (2013) Zwitterion vs neutral structures of amino acids stabilized by a negatively charged site: infrared photodissociation and computations of proline-chloride anion. J Phys Chem A 117:4863–4869
88. Prell JS, Correra TC, Chang TM, Biles JA, Williams ER (2010) Entropy drives an attached water molecule from the C- to N-terminus on protonated proline. J Am Chem Soc 132: 14733–14735
89. Prell JS, Chang TM, O'Brien JT, Williams ER (2010) Hydration isomers of protonated phenylalanine and derivatives: relative stabilities from infrared photodissociation. J Am Chem Soc 132:7811–7819
90. Verkerk UH, Zhao JF, Saminathan IS, Lau JKC, Oomens J, Hopkinson AC, Siu KWM (2012) Infrared multiple-photon dissociation spectroscopy of tripositive ions: lanthanum-tryptophan complexes. Inorg Chem 51:4707–4710
91. Fridgen TD, MacAleese L, Maître P, McMahon TB, Boissel P, Lemaire J (2005) Infrared spectra of homogeneous and heterogeneous proton-bound dimers in the gas phase. PCCP 7: 2747–2755
92. Fridgen TD, MacAleese L, McMahon TB, Lemaire J, Maître P (2006) Gas phase infrared multiple-photon dissociation spectra of methanol, ethanol and propanol proton-bound dimers, protonated propanol and the propanol/water proton-bound dimer. PCCP 8:955–966
93. Rajabi K, Fridgen TD (2008) Structures of aliphatic amino acid proton-bound dimers by infrared multiple photon dissociation spectroscopy in the 700–2000 cm(−1) region. J Phys Chem A 112:23–30
94. Wu RH, Marta RA, Martens JK, Eldridge KR, McMahon TB (2011) Experimental and theoretical investigation of the proton-bound dimer of lysine. J Am Soc Mass Spectrom 22: 1651–1659
95. Wu RH, McMahon TB (2007) Infrared multiple photon dissociation spectra of proline and glycine proton-bound homodimers. Evidence for zwitterionic structure. J Am Chem Soc 129: 4864–4865
96. Steill JD, Szczepanski J, Oomens J, Eyler JR, Brajter-Toth A (2011) Structural characterization by infrared multiple photon dissociation spectroscopy of protonated gas-phase ions obtained by electrospray ionization of cysteine and dopamine. Anal Bioanal Chem 399: 2463–2473
97. Atkins CG, Rajabi K, Gillis EAL, Fridgen TD (2008) Infrared multiple photon dissociation spectra of proton- and sodium ion-bound glycine dimers in the N-H and O-H stretching region. J Phys Chem A 112:10220–10225
98. Dunbar RC, Steill JD, Polfer NC, Oomens J (2009) Dimeric complexes of tryptophan with M^{2+} metal ions. J Phys Chem A 113:845–851
99. Mino WK, Szczepanski J, Pearson WL, Powell DH, Dunbar RC, Eyler JR, Polfer NC (2010) Vibrational signatures of zwitterionic and charge-solvated structures for alkaline earth-tryptophan dimer complexes in the gas phase. Int J Mass Spectrom 297:131–138

100. Balaj OP, Kapota C, Lemaire J, Ohanessian G (2008) Vibrational signatures of sodiated oligopeptides (GG-Na+, GGG-Na+, AA-Na + and AAA-Na+) in the gas phase. Int J Mass Spectrom 269:196–209
101. Dunbar RC, Steill JD, Oomens J (2011) Encapsulation of metal cations by the PhePhe ligand: a cation-π ion cage. J Am Chem Soc 133:9376–9386
102. Prell JS, Demireva M, Oomens J, Williams ER (2009) Role of sequence in salt-bridge formation for alkali metal cationized GlyArg and ArgGly investigated with IRMPD spectroscopy and theory. J Am Chem Soc 131:1232–1242
103. Dunbar RC, Steill JD, Oomens J (2011) Chirality-induced conformational preferences in peptide-metal ion binding revealed by IR spectroscopy. J Am Chem Soc 133:1212–1215
104. Dunbar RC, Steill JD, Oomens J (2010) Conformations and vibrational spectroscopy of metal ion/polylalanine complexes. Int J Mass Spectrom 297:107–115
105. Balaj OP, Semrouni D, Steinmetz V, Nicol E, Clavaguera C, Ohanessian G (2012) Structure of sodiated polyglycines. Chem Eur J 18:4583–4592
106. Dunbar RC, Steill JD, Polfer NC, Oomens J (2013) Metal cation binding to gas-phase pentaalanine: divalent ions restructure the complex. J Phys Chem A 117:1094–1101
107. Dunbar RC, Polfer NC, Berden G, Oomens J (2012) Metal ion binding to peptides: oxygen or nitrogen sites? Int J Mass Spectrom 330–332:71–77
108. Wyttenbach T, Liu D, Bowers MT (2008) Interactions of the hormone oxytocin with divalent metal ions. J Am Chem Soc 130:5993–6000
109. Dunbar RC, Steill JD, Polfer NC, Berden G, Oomens J (2012) Peptide bond tautomerization induced by divalent metal ions: characterization of the iminol configuration. Angew Chem Int Ed 51:4591–4593
110. Dunbar RC, Oomens J, Berden G, Lau JKC, Verkerk UH, Hopkinson AC, Siu KWM (2013) Metal ion complexes with HisGly: comparison with PhePhe and PheGly. J Phys Chem A 117: 5335–5343
111. Martin RB (1990) In: Sigel A, Sigel H (eds) Magnesium and its role in biology. Nutrition and physiology. Marcel Dekker, New York, pp 1–13
112. Martin RB (1984) In: Sigel A, Sigel H (eds) Metal ions in biological systems: probing of proteins by metal ions and their low-molecular-weight complexes. Marcel Dekker, New York, pp 1–49
113. Andrews RK, Blakely RL, Zerner B (1988) In: Sigel A, Sigel H (eds) Metal ions in biological systems: nickel and its role in biology. Marcel Dekker, New York, pp 165–284
114. Martin RB (1988) In: Sigel A, Sigel H (eds) Metal ions in biological systems: nickel and its role in biology. Marcel Dekker, New York, pp 123–164
115. Sovago I, Osz K (2006) Metal ion selectivity of oligopeptides. Dalton Trans 3841–3854
116. Dunbar RC, Steill JD, Polfer NC, Oomens J (2013) Metal cation binding to gas-phase pentaalanine: divalent ions restructure the complex. J Phys Chem A 117(6):1094–1101
117. Semrouni D, Balaj OP, Calvo F, Correia CF, Clavaguera C, Ohanessian G (2010) Structure of sodiated octa-glycine: IRMPD spectroscopy and molecular modeling. J Am Soc Mass Spectrom 21:728–738
118. Semrouni D, Clavaguera C, Dognon JP, Ohanessian G (2010) Assessment of density functionals for predicting the infrared spectrum of sodiated octa-glycine. Int J Mass Spectrom 297:152–161
119. Martens JK, Compagnon I, Nicol E, McMahon TB, Clavaguera C, Ohanessian G (2012) Globule to helix transition in sodiated polyalanines. J Phys Chem Lett 3:3320–3324
120. Kupser P, Pagel K, Oomens J, Polfer N, Koksch B, Meijer G, von Helden G (2010) Amide-I and -II vibrations of the cyclic beta-sheet model peptide gramicidin S in the gas phase. J Am Chem Soc 132:2085–2093
121. Nagornova NS, Rizzo TR, Boyarkin OV (2010) Highly resolved spectra of gas-phase gramicidin S: a benchmark for peptide structure calculations. J Am Chem Soc 132:4040

122. Nagornova NS, Guglielmi M, Doemer M, Tavernelli I, Rothlisberger U, Rizzo TR, Boyarkin OV (2011) Cold-ion spectroscopy reveals the intrinsic structure of a decapeptide. Angew Chem Int Ed 50:5383–5386
123. Bush MF, Prell JS, Saykally RJ, Williams ER (2007) One water molecule stabilizes the cationized arginine zwitterion. J Am Chem Soc 129:13544–13553
124. Schmidt J, Meyer MM, Spector I, Kass SR (2011) Infrared multiphoton dissociation spectroscopy study of protonated p-aminobenzoic acid: does electrospray ionization afford the amino- or carboxy-protonated ion? J Phys Chem A 115:7625–7632
125. Tian ZX, Kass SR (2009) Gas-phase versus liquid-phase structures by electrospray ionization mass spectrometry. Angew Chem Int Ed 48:1321–1323
126. Schroder D, Budesinsky M, Roithova J (2012) Deprotonation of p-hydroxybenzoic acid: does electrospray ionization sample solution or gas-phase structures? J Am Chem Soc 134: 15897–15905
127. Tian ZX, Kass SR (2008) Does electrospray ionization produce gas-phase or liquid-phase structures? J Am Chem Soc 130:10842–10843
128. Tian ZX, Wang XB, Wang LS, Kass SR (2009) Are carboxyl groups the most acidic sites in amino acids? Gas-phase acidities, photoelectron spectra, and computations on tyrosine, p-hydroxybenzoic acid, and their conjugate bases. J Am Chem Soc 131:1174–1181
129. Steill JD, Oomens J (2009) Gas-phase deprotonation of p-hydroxybenzoic acid investigated by IR spectroscopy: solution-phase structure is retained upon ESI. J Am Chem Soc 131: 13570
130. Rogalewicz F, Hoppilliard Y, Ohanessian G (2003) Structures and fragmentations of zinc(II) complexes of amino acids in the gas phase – IV. Solvent effect on the structure of electrosprayed ions. Int J Mass Spectrom 227:439–451
131. Tanabe K, Miyazaki M, Schmies M, Patzer A, Schutz M, Sekiya H, Sakai M, Dopfer O, Fujii M (2012) Watching water migration around a peptide bond. Angew Chem Int Ed 51: 6604–6607
132. Lifshitz C (1997) Energetics and dynamics through time-resolved measurements in mass spectrometry: aromatic hydrocarbons, polycyclic aromatic hydrocarbons and fullerenes. Int Rev Phys Chem 16:113–139
133. Orth R, Dunbar RC, Riggin M (1977) Measurement of angular-distribution and energy of ionic fragments from photodissociation of molecular-ions. Chem Phys 19:279–288
134. Bellina B, Compagnon I, Joly L, Albrieux F, Allouche AR, Bertorelle F, Lemoine J, Antoine R, Dugourd P (2010) UV spectroscopy of entire proteins in the gas phase. Int J Mass Spectrom 297:36–40
135. Bellina B, Compagnon I, MacAleese L, Chirot F, Lemoine J, Maître P, Broyer M, Antoine R, Kulesza A, Mitric R, Bonacic-Koutecky V, Dugourd P (2012) Binding motifs of silver in prion octarepeat model peptides: a joint ion mobility, IR and UV spectroscopies, and theoretical approach. PCCP 14:11433–11440
136. Brunet C, Antoine R, Lemoine J, Dugourd P (2012) Soret band of the gas-phase ferricytochrome c. J Phys Chem Lett 3:698–702
137. Bellina B, Compagnon I, Bertorelle F, Broyer M, Antoine R, Dugourd P, Gell L, Kulesza A, Mitric R, Bonacic-Koutecky V (2011) Structural and optical properties of isolated noble metal-glutathione complexes: insight into the chemistry of liganded nanoclusters. J Phys Chem C 115:24549–24554
138. Antoine R, Bertorelle F, Broyer M, Compagnon I, Dugourd P, Kulesza A, Mitric R, Bonacic-Koutecky V (2009) Gas-phase synthesis and intense visible absorption of tryptophan-gold cations. Angew Chem Int Ed 48:7829–7832
139. Bellina B, Compagnon I, Houver S, Maître P, Allouche AR, Antoine R, Dugourd P (2011) Spectroscopic signatures of peptides containing tryptophan radical cations. Angew Chem Int Ed 50:11430–11432

140. Joly L, Antoine R, Albrieux F, Ballivian R, Broyer M, Chirot F, Lemoine J, Dugourd P, Greco C, Mitric R, Bonacic-Koutecky V (2009) Optical and structural properties of copper-oxytocin dications in the gas phase. J Phys Chem B 113:11293–11300
141. Joly L, Antoine R, Allouche AR, Broyer M, Lemoine J, Dugourd P (2009) Optical properties of isolated hormone oxytocin dianions: ionization, reduction, and copper complexation effects. J Phys Chem A 113:6607–6611
142. Kirk BB, Trevitt AJ, Blanksby SJ, Tao Y, Moore BN, Julian RR (2013) Ultraviolet action spectroscopy of iodine labeled peptides and proteins in the gas phase. J Phys Chem A 117: 1228–1232
143. Ly T, Julian RR (2010) Elucidating the tertiary structure of protein ions in vacuo with site specific photoinitiated radical reactions. J Am Chem Soc 132:8602–8609
144. Ly T, Julian RR (2009) Ultraviolet photodissociation: developments towards applications for mass-spectrometry-based proteomics. Angew Chem Int Ed 48:7130–7137
145. Enjalbert Q, Brunet C, Vernier A, Allouche AR, Antoine R, Dugourd P, Lemoine J, Giuliani A, Nahon L (2013) Vacuum ultraviolet action spectroscopy of polysaccharides. J Am Soc Mass Spectrom 24:1271–1279